MR No. L5A29a

NATIONAL ADVISORY COMMITTEE FOR AERONAUTICS

WARTIME REPORT

ORIGINALLY ISSUED
January 1945 as
Memorandum Report L5A29a

MEASUREMENT OF INDIVIDUAL AILERON HINGE MOMENTS AND AILERON CONTROL CHARACTERISTICS OF A P-40F AIRPLANE

By R. Fabian Goranson

Langley Memorial Aeronautical Laboratory
Langley Field, Va.

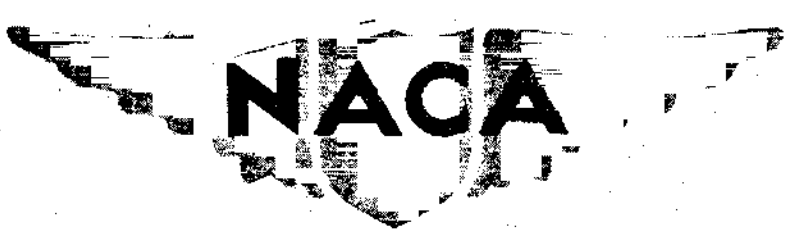

WASHINGTON

NACA WARTIME REPORTS are reprints of papers originally issued to provide rapid distribution of advance research results to an authorized group requiring them for the war effort. They were previously held under a security status but are now unclassified. Some of these reports were not technically edited. All have been reproduced without change in order to expedite general distribution.

NATIONAL ADVISORY COMMITTEE FOR AERONAUTICS

MEMORANDUM REPORT

for the

Army Air Forces, Air Technical Service Command

MEASUREMENT OF INDIVIDUAL AILERON HINGE MOMENTS AND AILERON CONTROL CHARACTERISTICS OF A P-40F AIRPLANE

By R. Fabian Goranson

SUMMARY

Flight measurements have been made of the individual aileron hinge moments, aileron rolling effectiveness pb/2V, and stick-force characteristics in abrupt aileron rolls with a P-40F airplane (AAF No. 41-14119) over an indicated airspeed range from 108 to 304 miles per hour. Three methods for measuring the rate of change of hinge moment with angle of attack were investigated. Presented for comparison with the flight results are data from two-dimensional wind-tunnel tests of the wing-aileron profile as measured at the center aileron hinge.

These measured characteristics of the P-40F standard ailerons show that these ailerons produced a helix angle pb/2V of 0.08 radian at 200 miles per hour, but that the elastic control system reduced the maximum helix angle to 0.06 with full stick deflection at 300 miles per hour. Stick forces were objectionably unsymmetrical to left and right. Hinge-moment measurements show that the flight measured values were approximately 40 to 60 percent of the value indicated by two-dimensional tests with the largest difference appearing at high aileron deflections. Another point worth noting is that flight tests also showed that the ailerons were effective to approximately 2° higher deflection than indicated by the wind-tunnel tests. This comparison between flight and wind-tunnel data indicates the need to evaluate the lifting-surface theory and thereby provide the numerical quantities necessary to correct section data for plan-form effects when estimating stick forces for a finite aileron-wing combination.

INTRODUCTION

The program for the development of satisfactory ailerons for the XP-75 airplane, which employs the P-40 wing as its outboard panel, consisted of two-dimensional wind-tunnel tests in the Langley stability tunnel and flight tests with a P-40F airplane. Wind-tunnel tests were made with models of the wing-aileron profile as measured at the center aileron hinge.

Although there were a few data available on aileron hinge moments measured in flight, there were no data which were comparable to two-dimensional wind-tunnel tests. It was therefore advantageous to investigate the effectiveness and hinge-moment characteristics of the standard P-40F ailerons in flight and in the wind tunnel in order to provide data to check current theories for correcting section data to the free-flight condition. In addition, the flight tests would provide a basis for evaluating the characteristics of the XP-75 ailerons, permit investigation and perfection of techniques for measuring hinge-moment characteristics, and allow measurements of friction forces and stretch inherent in the P-40 control system.

The results of the P-40F standard aileron flight investigations are presented in this report.

DESCRIPTION OF THE TEST AIRPLANE AND INSTRUMENTATION

These tests were conducted with a P-40F airplane (AAF No. 41-14119) flown at an average gross weight of 7870 pounds with the center of gravity at approximately 28 percent mean aerodynamic chord, wheels retracted. Two photographs of the test airplane are shown in figures 1 and 2, a true view of the right wing giving pertinent wing dimensions is presented in figure 3, and section views showing the aileron-wing and aileron profiles are shown in figure 4. Although figure 3 shows the right wing and aileron, the location of the inset trimming tab on the left aileron is shown by a dotted line. The left aileron is not equipped with the fixed external tab shown on the right aileron. The aileron profiles (fig. 4(b)) were obtained from plaster casts of the actual ailerons and therefore include local surface details. Differences

between the two ailerons are primarily due to local fabric reinforcements and cover plates and usually extend for less than 6 inches spanwise on the aileron.

Pertinent airplane dimensions are listed below:

Wing area, square feet	236
Wing span, feet	37.3
Wing aspect ratio	5.95
Wing taper ratio	2.32
Aileron area aft of hinge line, square feet	7.04
Root mean square chord of area aft of hinge line, feet	1.03
Control-stick length, feet	1.76
Tab area, square feet:	
External tab, right aileron	0.12
Inset tab, left aileron	0.25
Aileron location, percent wing semispan:	
Inboard end	54.0
Outboard end	91.0

Instrumentation for these tests included the following standard NACA recording instruments synchronized by an NACA chronometric timer:

Airspeed
Roll turnmeter
Aileron position
Accelerometer (three-component)
Stick force
Galvanometer (aileron hinge-moment recorder)

In addition to the recording instruments the airplane was equipped with a sensitive indicating airspeed meter and an indicating free-air thermometer (resistance-bulb type).

The airspeed recorder and indicator were connected to the P-40F production airspeed head in order to avoid detrimental air-flow characteristics which may occur when external booms are mounted near the aileron. The airspeed installation was calibrated for position error and the thermometer for compressibility effects.

Aileron hinge moments were measured by cable-tension recorders calibrated in terms of aileron hinge moments. The cable-tension-recorder unit, shown in a three-view drawing (fig. 5) and in a photograph (fig. 6), consists essentially of a "C" shaped spring unit with electric strain gages mounted on the stressed shank so as to

measure cable tension as a function of strain in the shank. A sufficiently large number of strain gages were mounted on the unit so that the current changes could be measured directly with a microammeter without an intermediate amplifier. Because changes in aileron-stick linkage ratio occurred between the aileron and the point where the cable-tension recorder was mounted in the control cable, it was necessary to calibrate the cable-tension recorders in terms of aileron hinge moment for various aileron deflections.

During the high-speed tests, a 35-millimeter camera was installed so as to photograph the aileron fabric bulging. The camera was mounted in the compartment behind the pilot's seat and photographed the upper surface of the aileron through the fuselage opening normally used to fill the fuselage gas tank.

The aileron deflections were measured at the inboard end of the aileron and are therefore independent of stretch in the aileron control system. Twisting of the aileron under load is neglected, however.

The relationship between control-stick position and aileron position is shown in figure 7 for the no-load condition as measured on the ground. The stick forces due to friction in the control system for the no-load condition as shown in figure 8 indicate an average friction force of about $2\frac{1}{2}$ pounds with a sharp increase in friction force near full deflection.

DEFINITION OF SYMBOLS

$pb/2V$ helix angle described by wing tip during roll, radians

where

p angular velocity in roll, radians per second

b wing span, 37.3 feet

V true airspeed, feet per second

C_h aileron hinge-moment coefficient $(H/qS\bar{c})$

where

H	aileron hinge moment, positive when tending to rotate the trailing edge down, pound-feet
q	dynamic pressure $\left(\frac{1}{2}\rho V^2\right)$
S	aileron area aft of hinge line, 7.04 square feet
$\bar{c}$	root mean square chord of the area aft of the hinge line, 1.03 feet
V_i	indicated airspeed $\left(\sqrt{\frac{2q}{\rho}}\right)$
C_{h_α}	rate of change of aileron hinge-moment coefficient with angle of attack at a constant aileron deflection
C_{h_δ}	rate of change of aileron hinge-moment coefficient with aileron angle at a constant angle of attack
δ_a	angular aileron deflection with respect to the wing chord line, degrees, positive when the trailing edge is down

TEST PROCEDURE

The test program can be roughly divided into two parts: First, measurement of aileron rolling effectiveness, control-force and hinge-moment characteristics in abrupt aileron rolls made with controls locked in accordance with standard NACA procedure; second, tests to determine hinge-moment variations with angle of attack.

All flights were made with landing gear and flaps retracted and at power required for level flight or at rated power for speeds exceeding the maximum level-flight speed. An average pressure altitude of 10,000 feet was maintained throughout the tests.

Three methods for determining the variation of aileron hinge moment with angle of attack were investigated. Hinge moments were first measured in level flight throughout the speed range. Since the aileron trim angle was different from zero and varied with speed, the hinge

moment at zero deflection could not be measured directly, but this effect was circumvented by slowly moving the ailerons through neutral and measuring rolling velocity and hinge moments corresponding to zero aileron deflection. The change in angle of attack due to rolling was then considered to be the increment obtained at the aileron midspan. The second method investigated was that of making abrupt pull-ups and push-downs and measuring the hinge moment during the period of steady acceleration. The third method consisted of making abrupt aileron rolls out of accelerated turns.

Check calibration and repeated tests indicate that the measurements are within the following limits of accuracy:

Rolling velocity, p, radians per second	±0.03
Aileron angle, δ_a, degrees	±0.2
Aileron hinge moment, H, pound-feet	±1
Airspeed, miles per hour	±1
Stick forces, pounds	±0.5

The accuracy of the aileron hinge moments is based on a comparison between measured stick forces and stick forces computed from measured aileron hinge moments so that the proportion of the error due to each aileron is not determined. The scatter in hinge-moment and stick-force data is attributable to the friction in the control system, which in flight is apparently less than static friction because of relief due to continual vibration of the airplane.

The aileron characteristics at each of the test speeds were measured by repeated flights in order to provide an adequate check on the results.

RESULTS AND DISCUSSION

The aileron rolling effectiveness pb/2V and stick-force characteristics as measured in abrupt aileron rolls are presented in figures 9 through 14, and the hinge-moment coefficients measured at the time of steady rolling velocity are presented in figures 15 and 16 for the left and right aileron, respectively.

The stick-force variations with aileron angle (figs. 9 to 14) show a marked dissymmetry between left and right rolls; however, the asymmetric force gradient can be explained on the basis of the hinge moments and aileron-to-stick linkage-ratio variation with aileron deflection. That is, an inspection of figure 7 shows a very rapid increase in mechanical advantage of the stick over the downgoing aileron. This increase in mechanical advantage for a unit down deflection is greater than the increase in hinge-moment coefficient (figs. 15 and 16); consequently, nearly the entire stick force is due to the hinge moment of the upgoing aileron over which the stick has a decreasing mechanical advantage. The shapes of the hinge-moment-coefficient curves show a distinct difference between two supposedly identical ailerons with the right aileron exhibiting a greater up-floating tendency than the left aileron and also a more negative slope "C_{h_δ}" during roll. The hinge-moment-coefficient curves indicate clearly then that in right rolls the stick force will increase progressively with aileron deflection whereas in left rolls the stick forces will reach a steady or decreasing value after the left aileron exceeds approximately -8° deflection. This difference between the hinge-moment characteristics of the left and right aileron and consequent dissymmetry in stick forces for left and right rolls is not entirely attributable to any one factor; however, the geometric differences between the two ailerons (external trimming tab attached to the inboard end of the right aileron, slight differences in contour shown in figure 4(b) and slight differences in rigging) together with the unsymmetrical yawing during right and left rolls (shown in unpublished data) provide adequate reason for the differences.

Frise ailerons usually exhibit abrupt changes in hinge moments at high up deflections, because the overhanging balance protrudes into the airstream at an angle that causes the lower aileron surface to stall. In order to determine the deflection at which this stall occurs, the stick stops were removed for all rolls except those at 108 miles per hour. With the stops removed -23° deflection was available on the ground with no load. At 151 miles per hour it was not possible to stall the upgoing aileron at the maximum available deflection, but at 203 miles per hour a severe oscillation occurred when the aileron stalled. The point at which this aileron oscillation occurred is indicated by dashed lines on the

hinge-moment-coefficient and stick-force curves. At 252 and 304 miles per hour the aileron control system stretched so much that the stalling deflection could not be attained, but stick-force curves exhibited peculiarities at high deflections. At 250 miles per hour the stick-force and hinge-moment coefficients rose sharply as if to indicate incipient stalling without the buffeting that occurred at 203 miles per hour. At 304 miles per hour (fig. 13), the ailerons exhibited an abrupt change in stick force at the time maximum rolling velocity was attained; that is, the stick-force and hinge-moment variations with aileron deflection follow the solid curve then during the rolls suddenly decrease as is indicated by the dotted curve. Since this airplane exhibits low directional stability, this sudden change in stick force may be due to sideslip attained in the roll.

A summary of the rolling characteristics is presented in figure 14. From this figure it is apparent that the control system is very elastic and that this stretch reduces the $pb/2V$ from an average value of 0.08 at 200 miles per hour to 0.06 at 300 miles per hour with the stick fully deflected. It would be most desirable, both from the standpoint of effectiveness and stick forces, to eliminate the elasticity of this control system.

The marked changes in slope of the hinge-moment curves at high speed, together with pilot's comments that the aileron fabric was bulging, prompted an investigation to determine the fabric contour in flight. Contours at the center of one panel of the upper surface of the left aileron in rolls at 350 miles per hour are shown in figure 17. These contours were obtained from 35-millimeter motion pictures of the aileron. A typical picture is shown in figure 18. Since the contour of only one surface is known, no quantitative results are available, but it appears that the mean camber line deflects in a direction to increase the hinge moments.

The results of tests to determine the hinge-moment variation with angle of attack are presented in figures 19 through 21. The data for figure 19 were obtained from flights wherein the angle-of-attack change was obtained by varying the airspeed. The angle of attack was also changed by varying the normal acceleration at a constant airspeed. In figure 20 are presented the results obtained from acceleration changes due to abrupt pull-ups and push-downs and in figure 21 results from rolling out of

The stick-force variations with aileron angle (figs. 9 to 14) show a marked dissymmetry between left and right rolls; however, the asymmetric force gradient can be explained on the basis of the hinge moments and aileron-to-stick linkage-ratio variation with aileron deflection. That is, an inspection of figure 7 shows a very rapid increase in mechanical advantage of the stick over the downgoing aileron. This increase in mechanical advantage for a unit down deflection is greater than the increase in hinge-moment coefficient (figs. 15 and 16); consequently, nearly the entire stick force is due to the hinge moment of the upgoing aileron over which the stick has a decreasing mechanical advantage. The shapes of the hinge-moment-coefficient curves show a distinct difference between two supposedly identical ailerons with the right aileron exhibiting a greater up-floating tendency than the left aileron and also a more negative slope "C_{h_δ}" during roll. The hinge-moment-coefficient curves indicate clearly then that in right rolls the stick force will increase progressively with aileron deflection whereas in left rolls the stick forces will reach a steady or decreasing value after the left aileron exceeds approximately -8° deflection. This difference between the hinge-moment characteristics of the left and right aileron and consequent dissymmetry in stick forces for left and right rolls is not entirely attributable to any one factor; however, the geometric differences between the two ailerons (external trimming tab attached to the inboard end of the right aileron, slight differences in contour shown in figure 4(b) and slight differences in rigging) together with the unsymmetrical yawing during right and left rolls (shown in unpublished data) provide adequate reason for the differences.

Frise ailerons usually exhibit abrupt changes in hinge moments at high up deflections, because the overhanging balance protrudes into the airstream at an angle that causes the lower aileron surface to stall. In order to determine the deflection at which this stall occurs, the stick stops were removed for all rolls except those at 108 miles per hour. With the stops removed -23° deflection was available on the ground with no load. At 151 miles per hour it was not possible to stall the upgoing aileron at the maximum available deflection, but at 203 miles per hour a severe oscillation occurred when the aileron stalled. The point at which this aileron oscillation occurred is indicated by dashed lines on the

constant-speed accelerated turns. All angle-of-attack calculations were made with an estimated lift-curve slope C_{L_α} of 0.0738.

To obtain the data presented in figures 19(a) and 19(b), the airplane was trimmed in level flight over a speed range from 113 to 230 miles per hour and the ailerons moved slowly from left to right. It was then possible to obtain measurements (fig. 19(a)) of hinge moments as the airplane was rolling with small and equal angular velocities to left and right as well as two points ($\alpha = 2.4^\circ$ and 3.4°) at zero rolling velocity. In figure 19(b) hinge-moment coefficients are plotted as a function of the angle of attack as corrected for the increment of angle of attack at the center of the aileron due to rolls. These data are segregated according to increment of angle of attack due to rolling. The third set of data (fig. 19(c)) was obtained by plotting the hinge-moment coefficient at zero aileron deflection, obtained from figure 15, as a function of the angle of attack corresponding to the test airspeed. Effects of rolling are negligible in figure 19(c), because level-flight trim points are so very nearly at zero aileron deflection. The distribution of aileron trim angles near zero deflection was obtained by minor changes in rigging. The data of figure 19 indicate an average value of C_{h_α} of -0.0034 per degree.

It appears advantageous to vary the angle of attack by varying the normal acceleration rather than the airspeed, because under this condition it is possible to measure C_{h_α} independently of effects due to speed changes. Of the two methods for changing acceleration, pull-ups and push-downs (fig. 20) were found unsatisfactory with this airplane because the elastic control system permitted the ailerons to float away from neutral as the acceleration changed, thereby introducing hinge-moment effects due to aileron deflection. For an airplane with a rigid control system, pull-ups and push-downs would provide a simple method to obtain data on the angle-of-attack effect on hinge moments, aileron neutral.

The data presented in figure 21 were obtained by trimming the airplane in a steady turn and making abrupt aileron rolls out of the turn. These results are very incomplete in that data for only two angles of attack are available; furthermore, no aileron effectiveness or

sideslip data are available. Considerable sideslip was experienced due to the low directional stability of this airplane and it is not possible to determine the effects or magnitude of the sideslip because the instrumentation did not include a yaw vane. It therefore appears that the method of making rolls out of accelerated turns is the most promising way to obtain a measurement of C_{h_α} for the entire deflection range, but the data of figure 21 cannot be considered conclusive.

For comparative purposes, wind-tunnel data from two-dimensional tests in the Langley stability tunnel of the aileron-wing profile at the center hinge (fig. 4) are presented in figures 22 to 24. These tests employed a 1/2-scale model and were run at approximately 150 and 300 miles per hour; consequently, these data correspond to full-scale Mach number and one-half of full-scale Reynolds number. Hinge moments measured in flight when corrected only for the effects of rolling are approximately 40 to 60 percent of the value indicated by the two-dimensional data of figures 22 to 24 with the greatest differences appearing at high aileron deflections. The flight data also show that the ailerons are effective to approximately 2° greater up deflection than is shown by the wind-tunnel tests. Although numerical values for correcting C_{h_δ} when converting from two-dimensional to three-dimensional flow have not yet been evaluated, the difference between the wind-tunnel and flight test results are about what would be expected. Numerical values for correcting C_{h_α} have been evaluated, however, and do show good agreement between flight and tunnel results; that is, figure 24 shows a value of -0.0050 for C_{h_α}, and reference 1 indicates a correction of 0.0012 if section data are to be applied to the P-40F wing. The corrected value of C_{h_α}, -0.0038, is in good agreement with the measured value of -0.0034 obtained from figure 19.

CONCLUDING REMARKS

The results of this investigation, although not sufficiently complete to determine all the hinge-moment characteristics of the P-40F ailerons, have clearly indicated the feasibility of measuring aileron-hinge moments in flight. Furthermore, the two-dimensional wind-tunnel tests carried on in conjunction with the flight tests

have pointed out the necessity of more extensive flight investigations incorporating positive control of all variables so as to provide the data necessary for checking available methods used in correcting wind-tunnel data to the free-flight condition. Finally a comparison of the two-dimensional and flight data indicates that theoretical corrections to the value of C_{h_α} obtained from two-dimensional tests give relatively good agreement with the flight values and that the difference between the values of C_{h_δ} obtained in two-dimensional and three-dimensional tests is in the expected direction. The need is therefore indicated for extending the lifting-surface theory to provide numerical values for the basic aerodynamic induction factors necessary for correcting two-dimensional hinge moments to the three-dimensional free-flight condition.

Langley Memorial Aeronautical Laboratory
National Advisory Committee for Aeronautics
Langley Field, Va., January 29, 1945

REFERENCE

1. Swanson, Robert S., and Gillis, Clarence L.: Limitations of Lifting-Line Theory for Estimation of Aileron Hinge-Moment Characteristics. NACA CB No. 3L02, 1943.

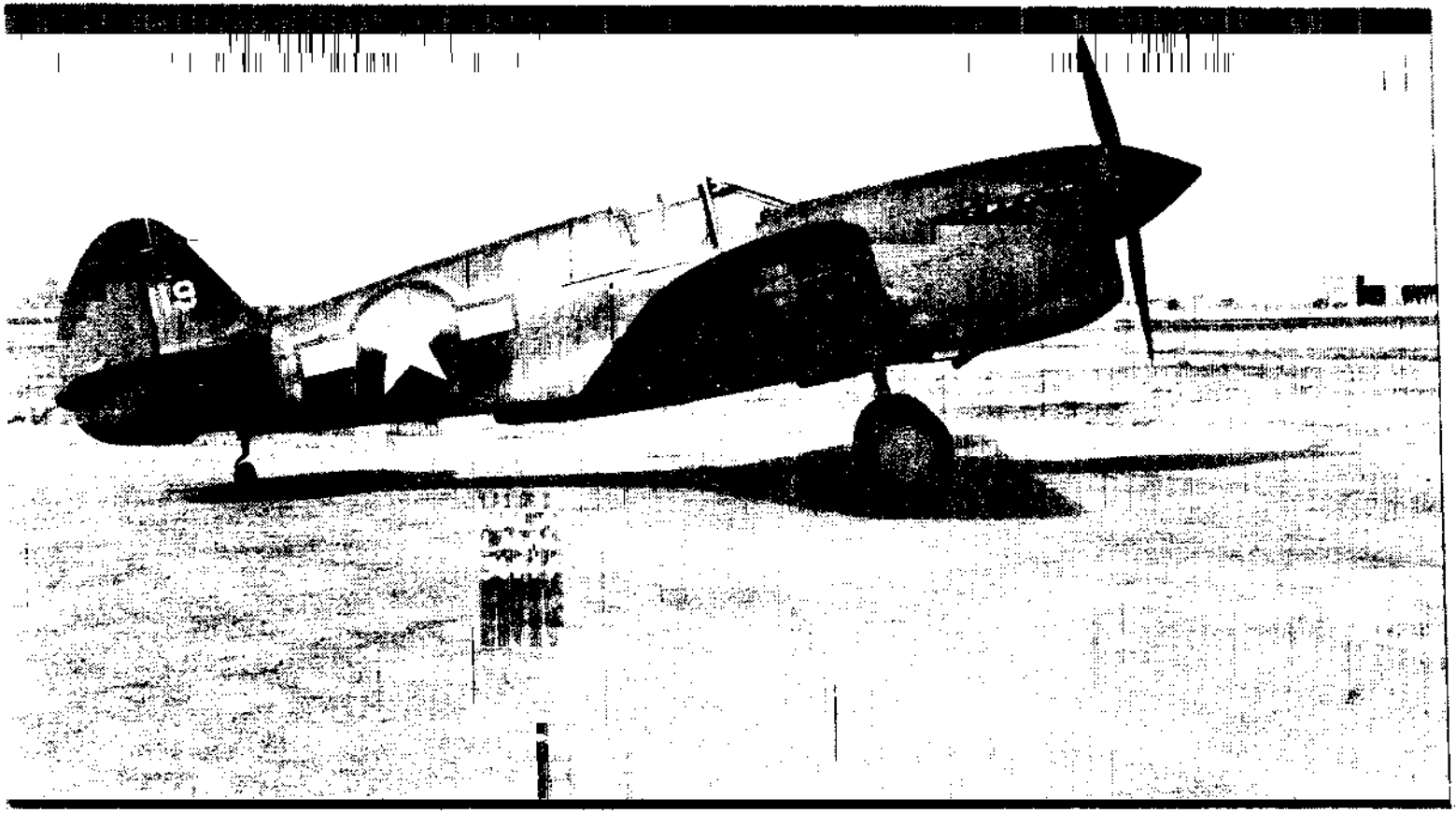

Figure 1.- Side view of the P-40F test airplane.

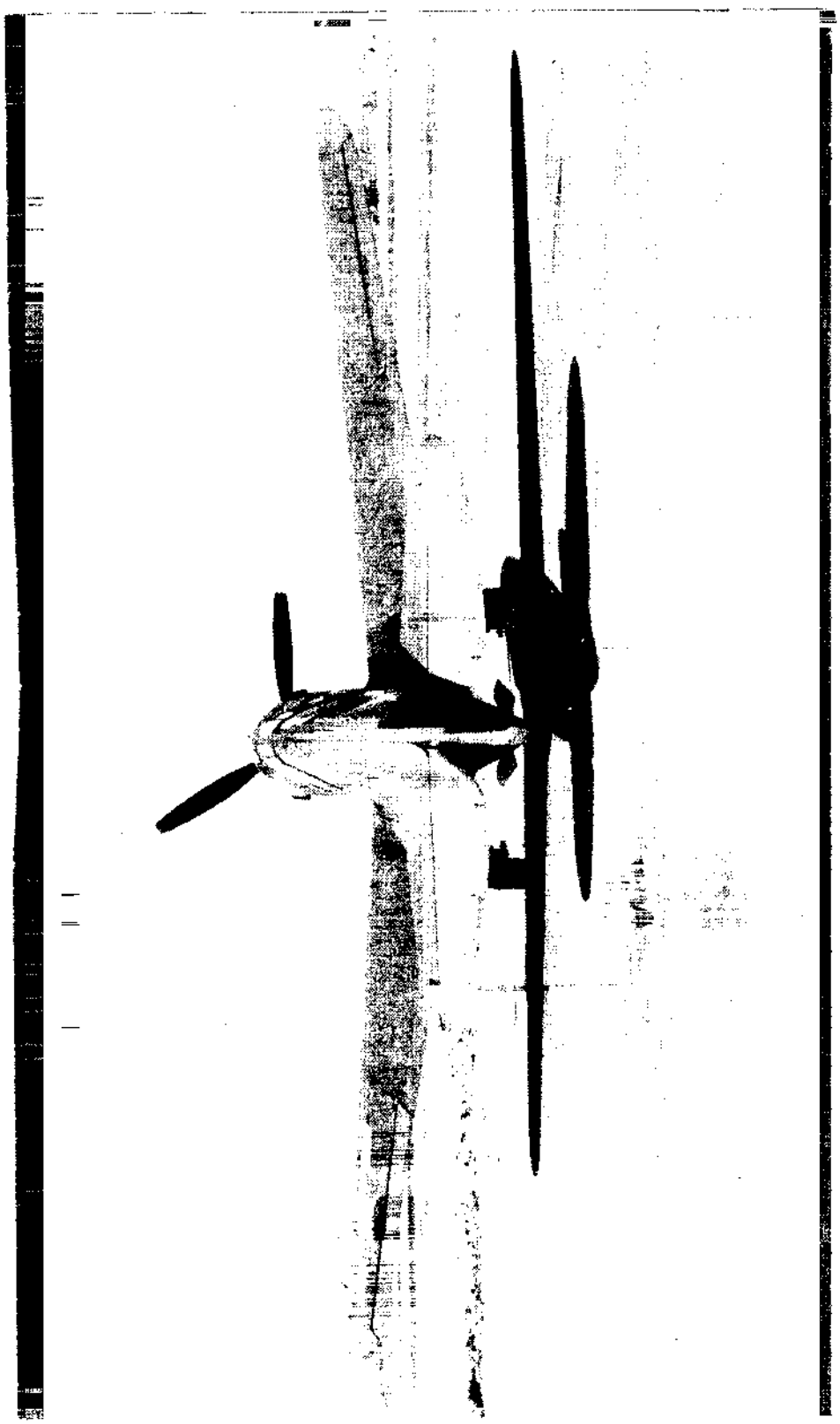

Figure 2.- Rear view of the P-40F test airplane.

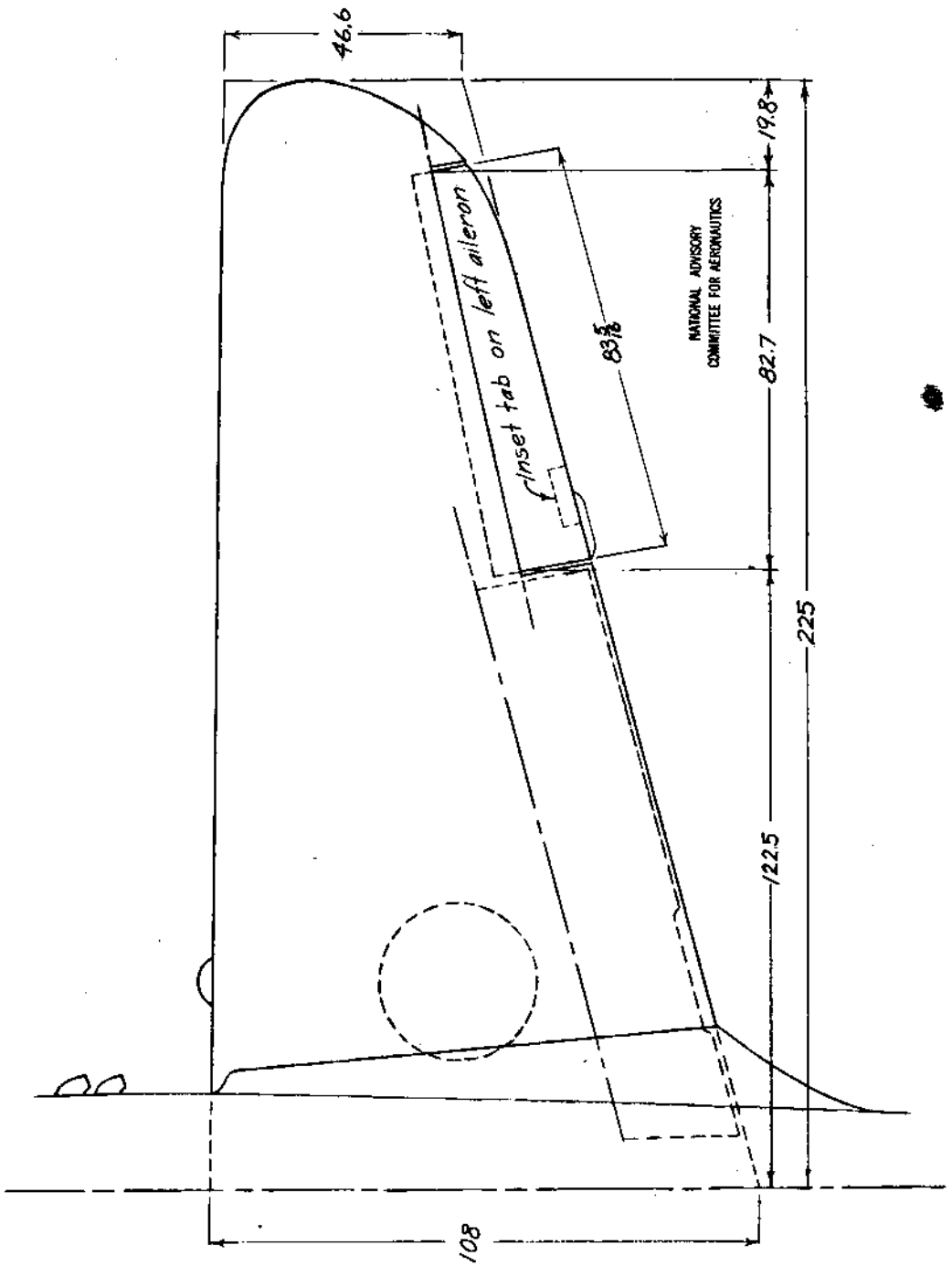

Figure 3. - True view of right wing of P-40F airplane.
All dimensions in inches.

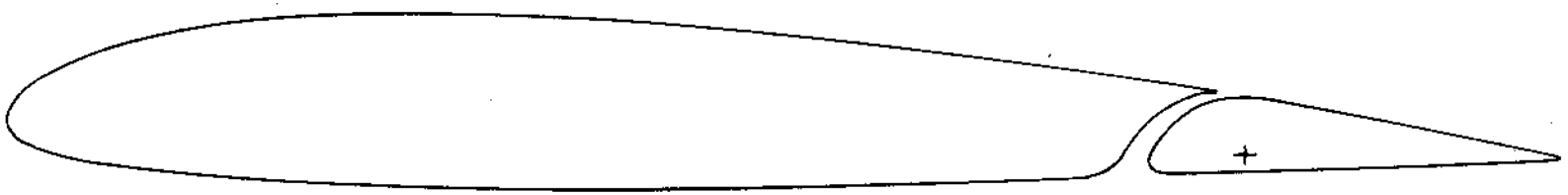

NATIONAL ADVISORY
COMMITTEE FOR AERONAUTICS

Figure 4 - Aileron and wing profiles.
(a) Aileron-wing profile at aileron center hinge, measured parallel to thrust axis.

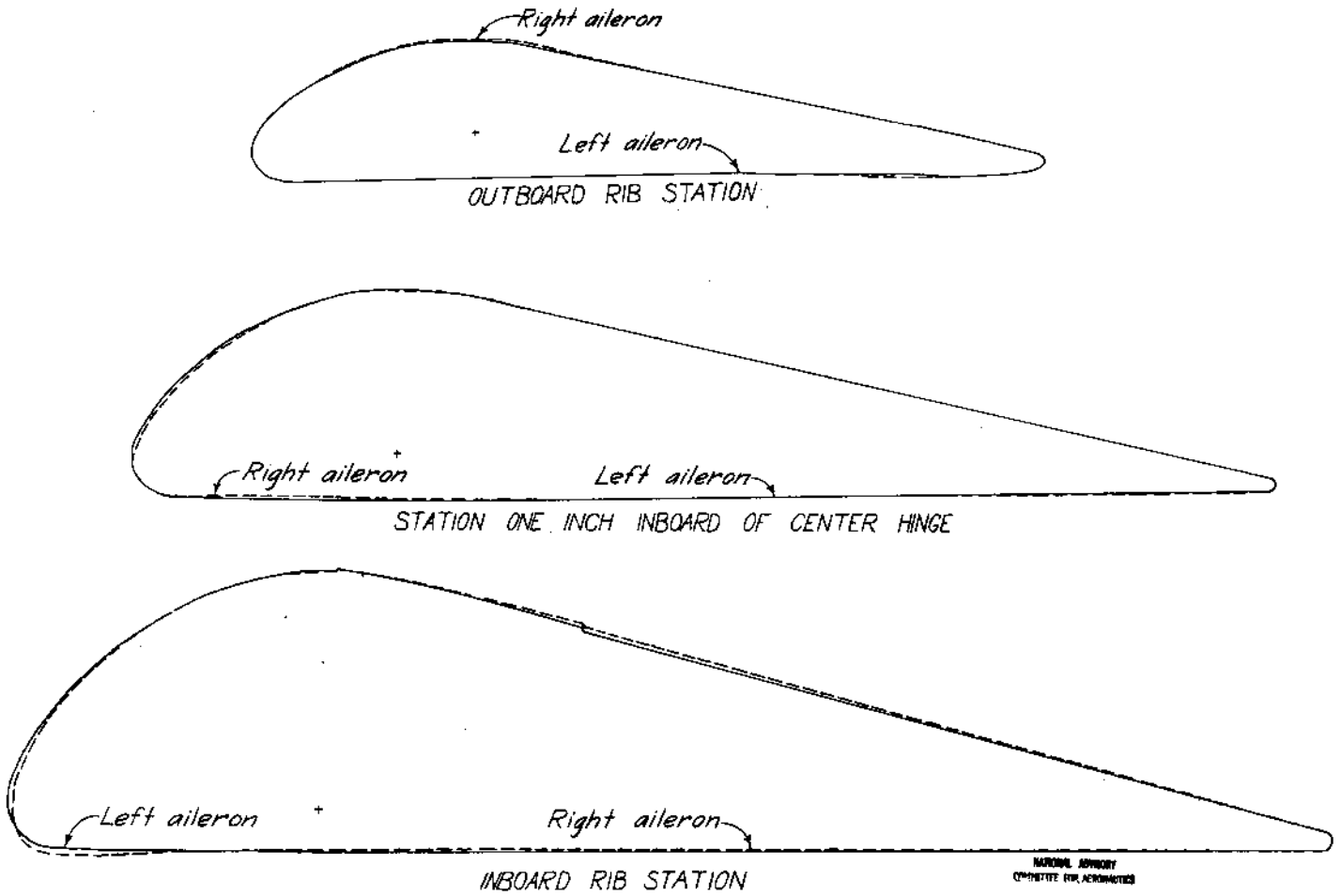

Figure 4- Concluded
(b) Aileron profiles measured perpendicular to the hinge line.

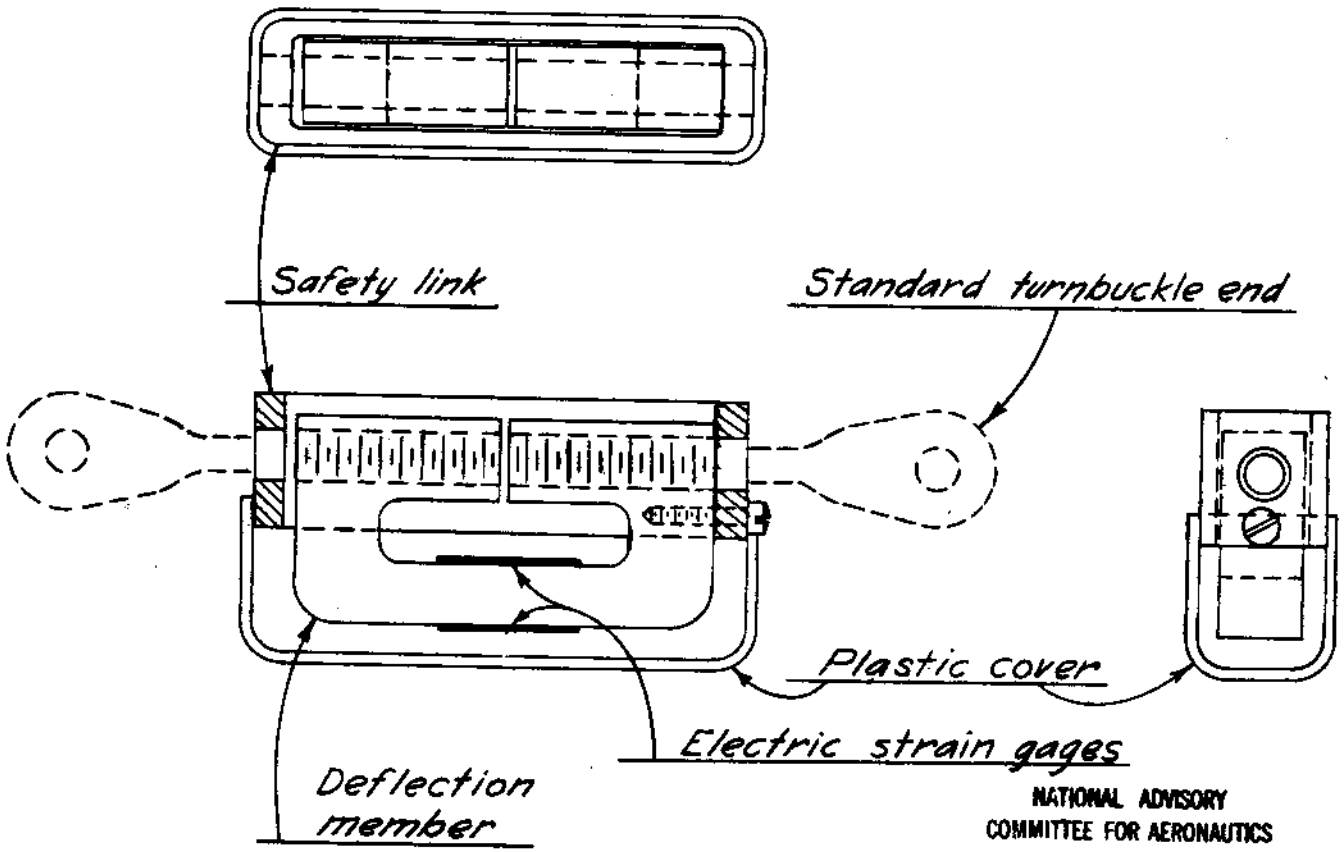

Figure 5 - Three-view drawing of cable-tension recorder unit.

L-649

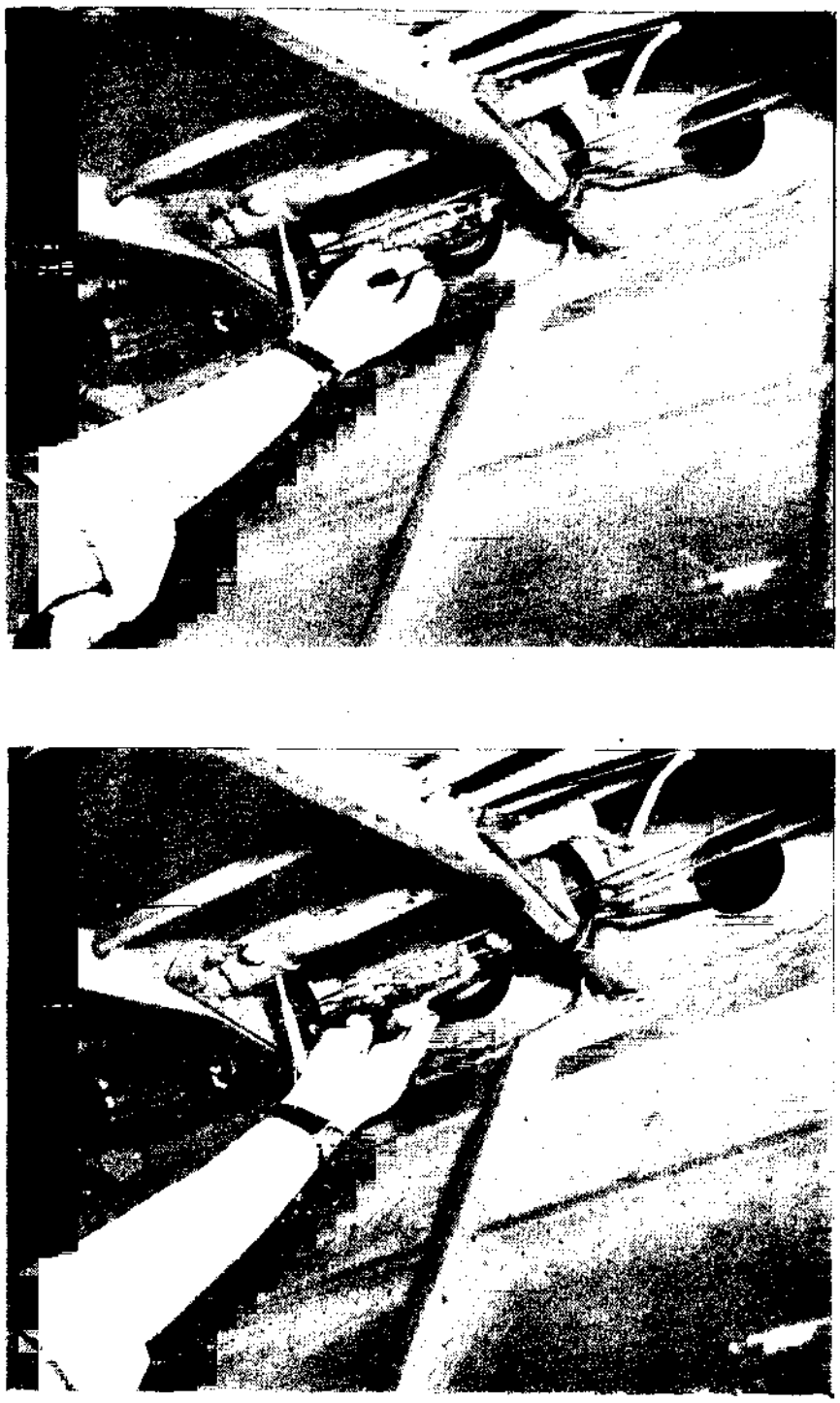

Figure 6.- Top and side view of the cable-tension unit used to measure the aileron hinge moments.

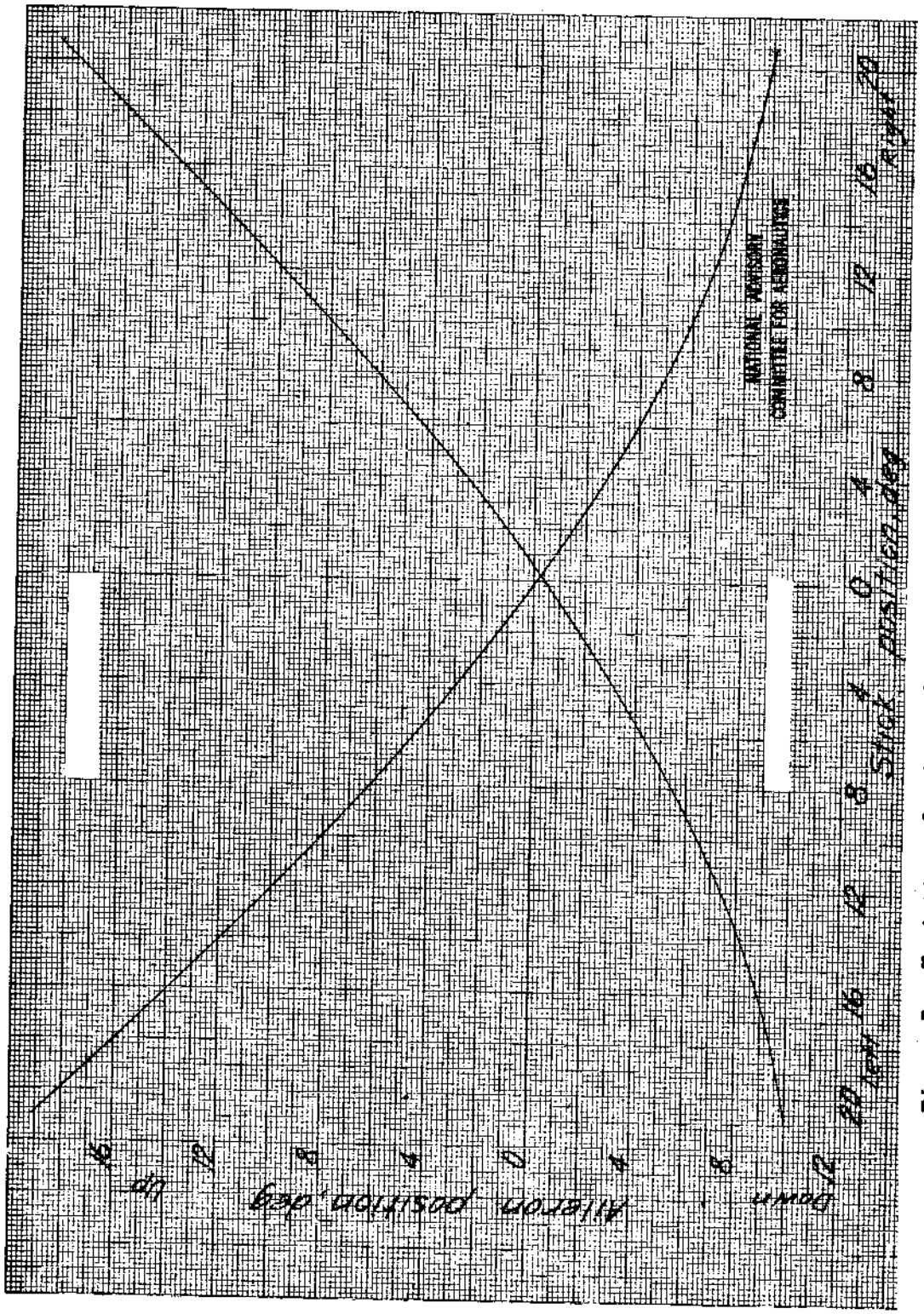

Figure 7 - Variation of aileron deflection with stick position for standard P-40F ailerons as measured on the ground with no aileron load.

L-649

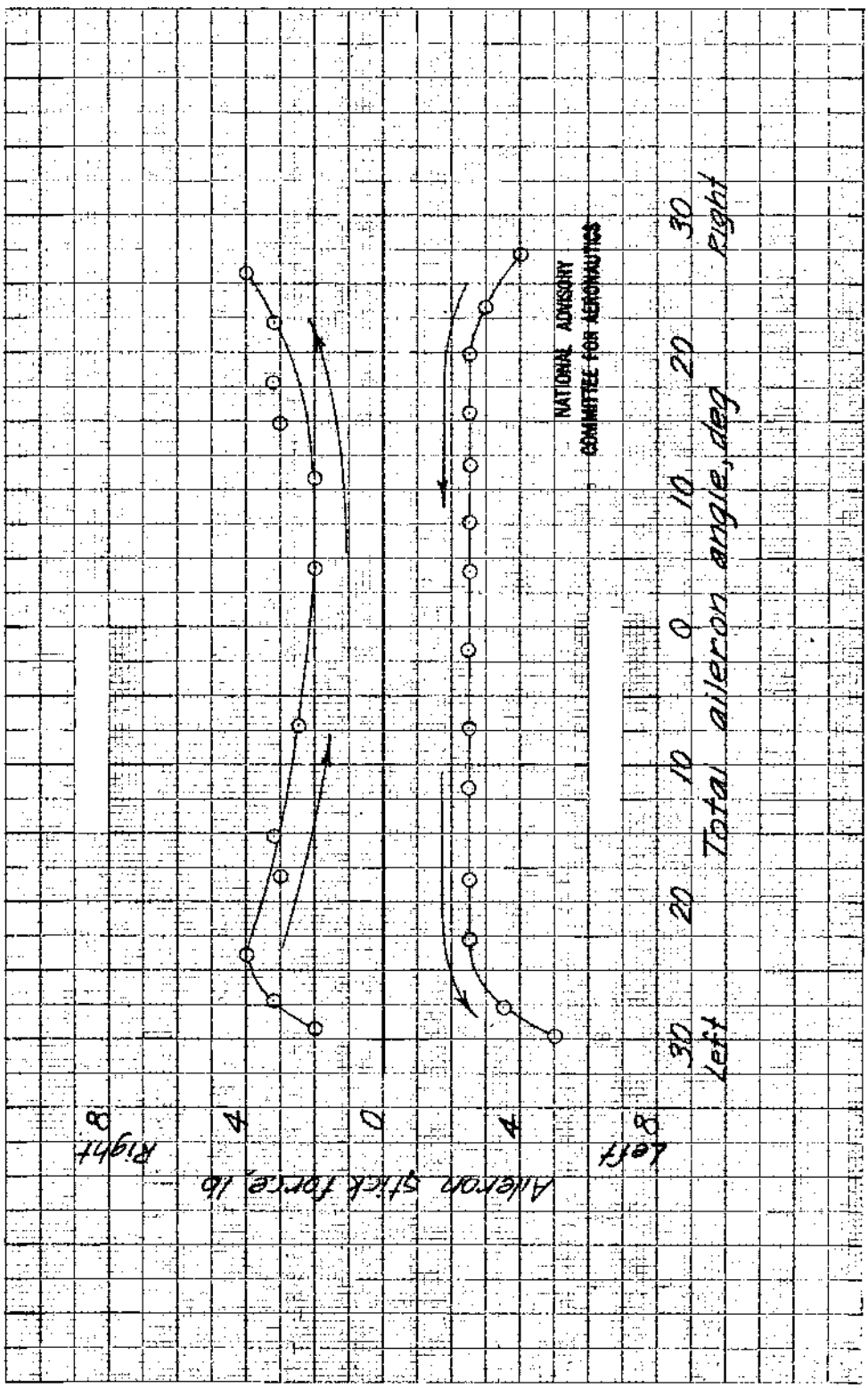

Figure 8 - Stick forces due to friction in the P-40F aileron control system as measured on the ground with no aileron load. Free air temperature 52° F.

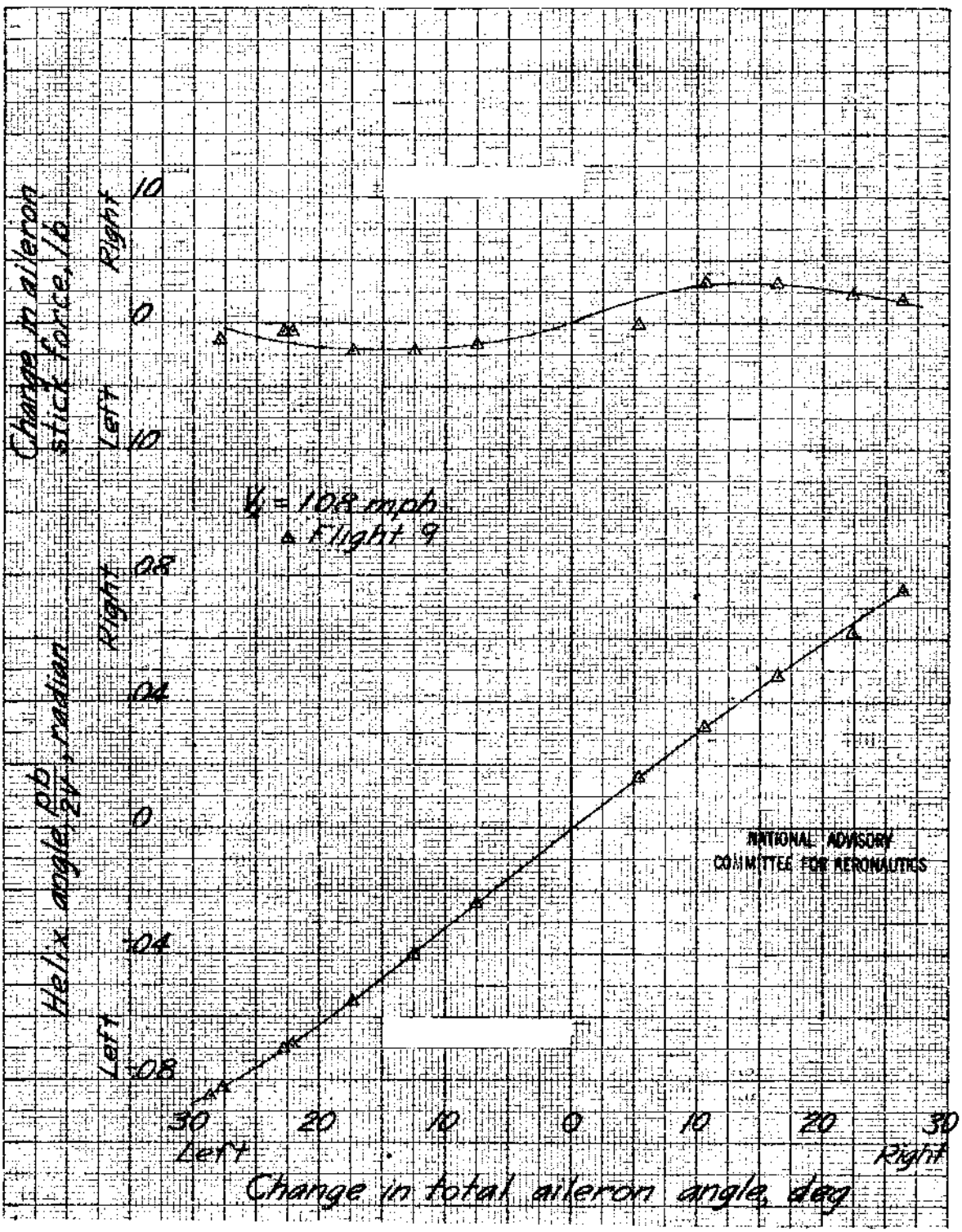

Figure 9 - Aileron rolling effectiveness and stick force characteristics of standard P-40F ailerons as measured in a steady roll at an average indicated airspeed of 108 miles per hour.

L-649

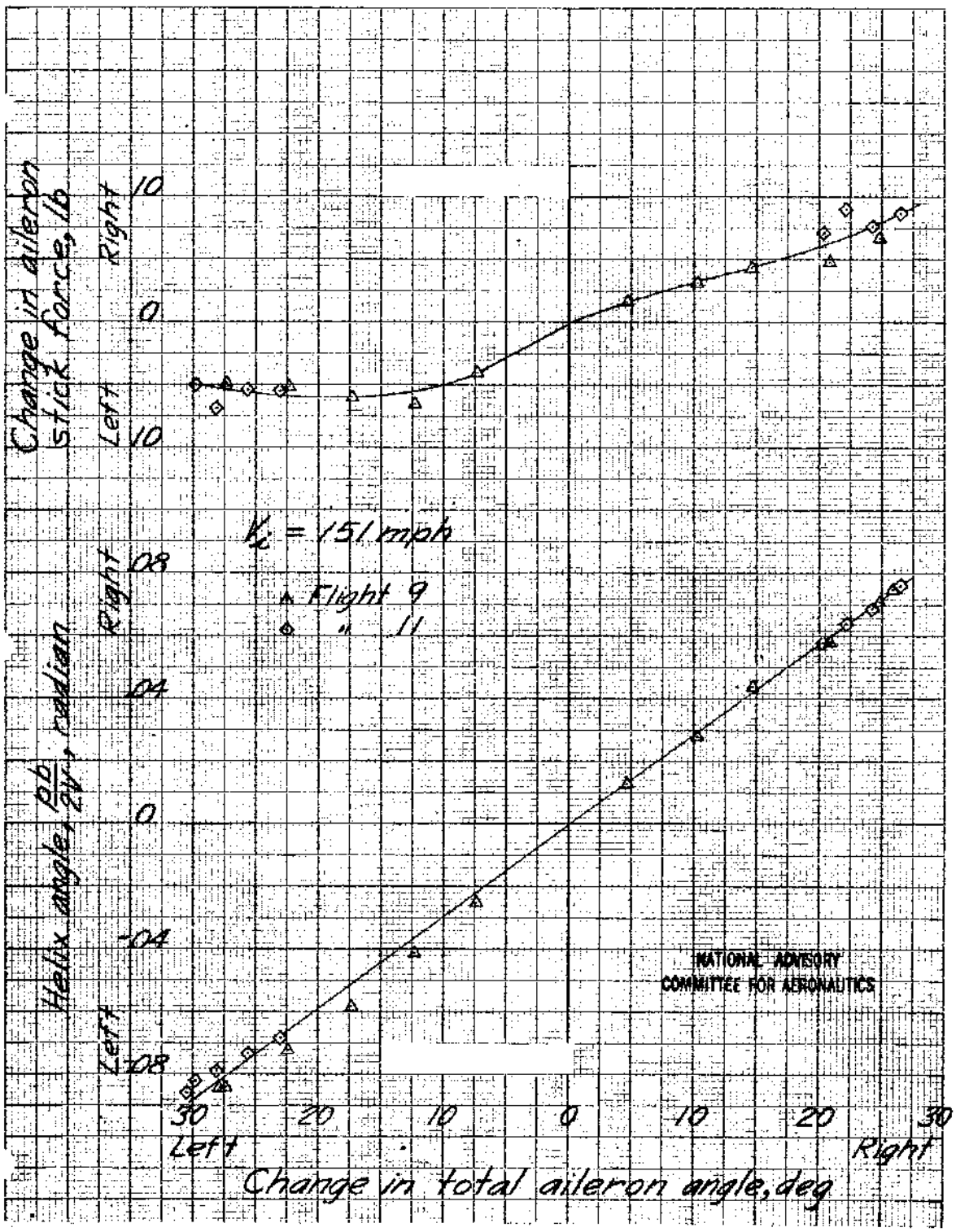

Figure 10 - Aileron rolling effectiveness and stick force characteristics of standard P-40F ailerons as measured in a steady roll at an average indicated airspeed of 151 miles per hour.

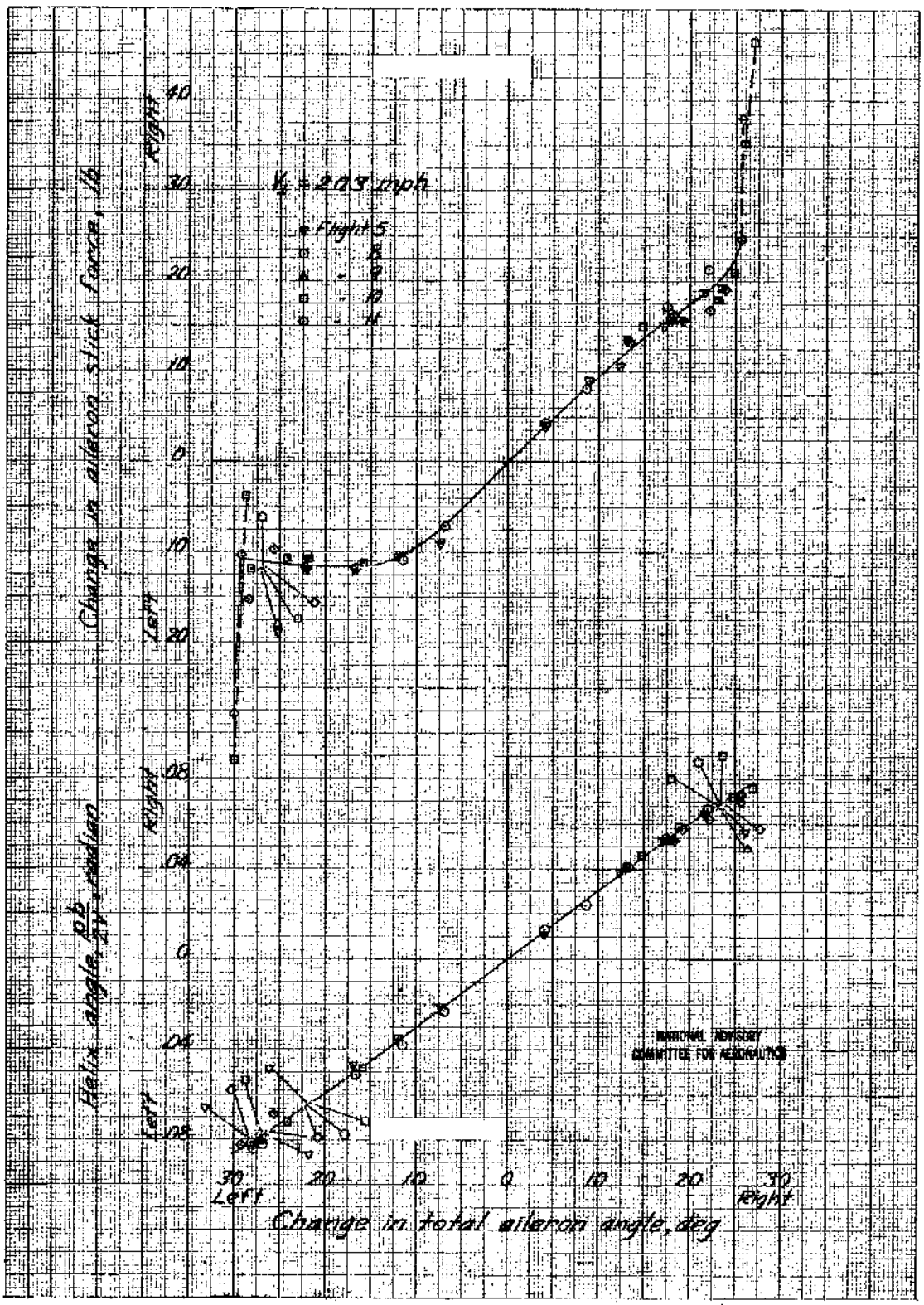

Figure 11 - Aileron rolling effectiveness and stick force characteristics of standard P-40F ailerons as measured in a steady roll at an average indicated airspeed of 203 miles per hour.

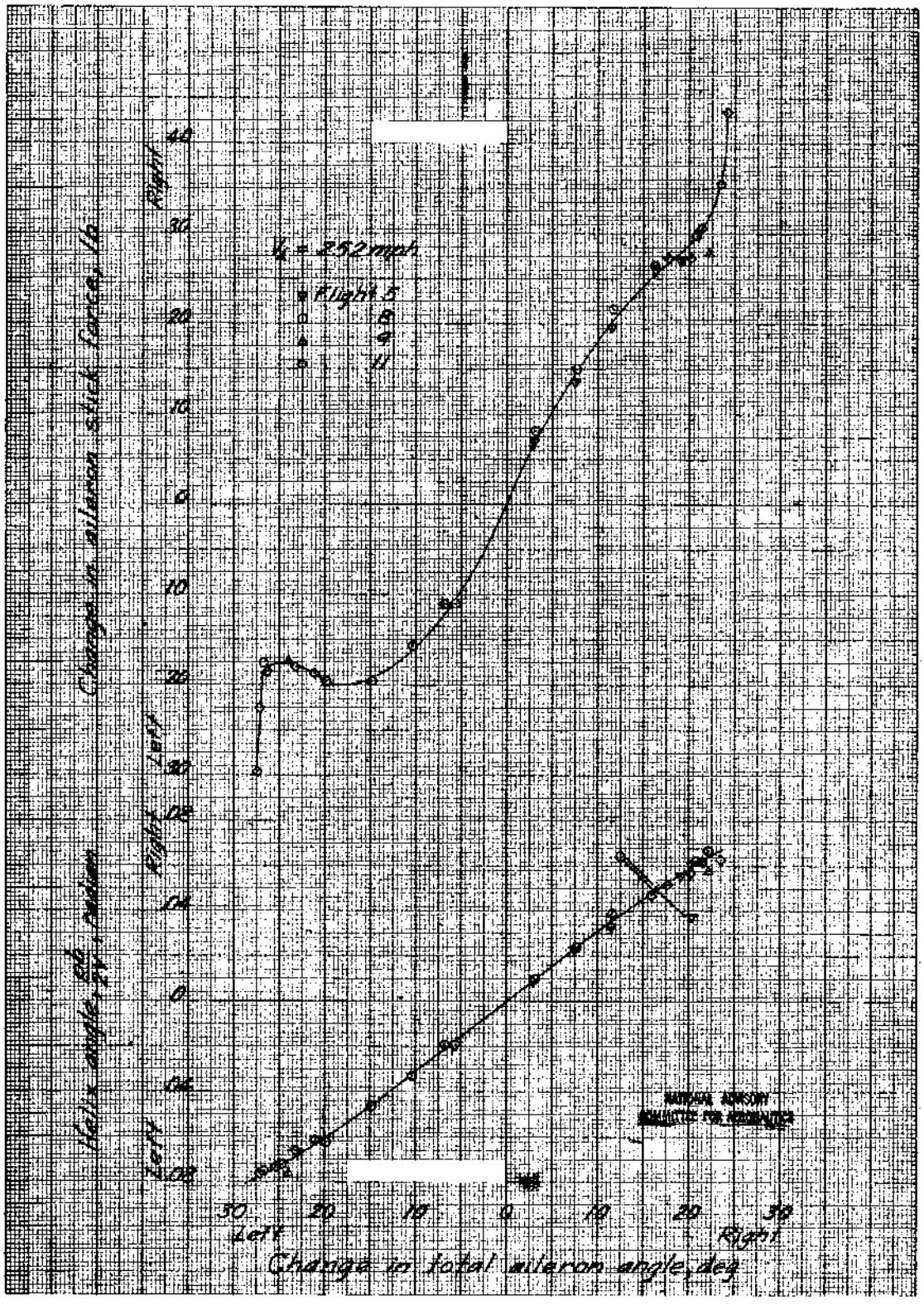

Figure 12 - Aileron rolling effectiveness and stick force characteristics of standard P-40F ailerons as measured in a steady roll at an average indicated airspeed of 252 miles per hour.

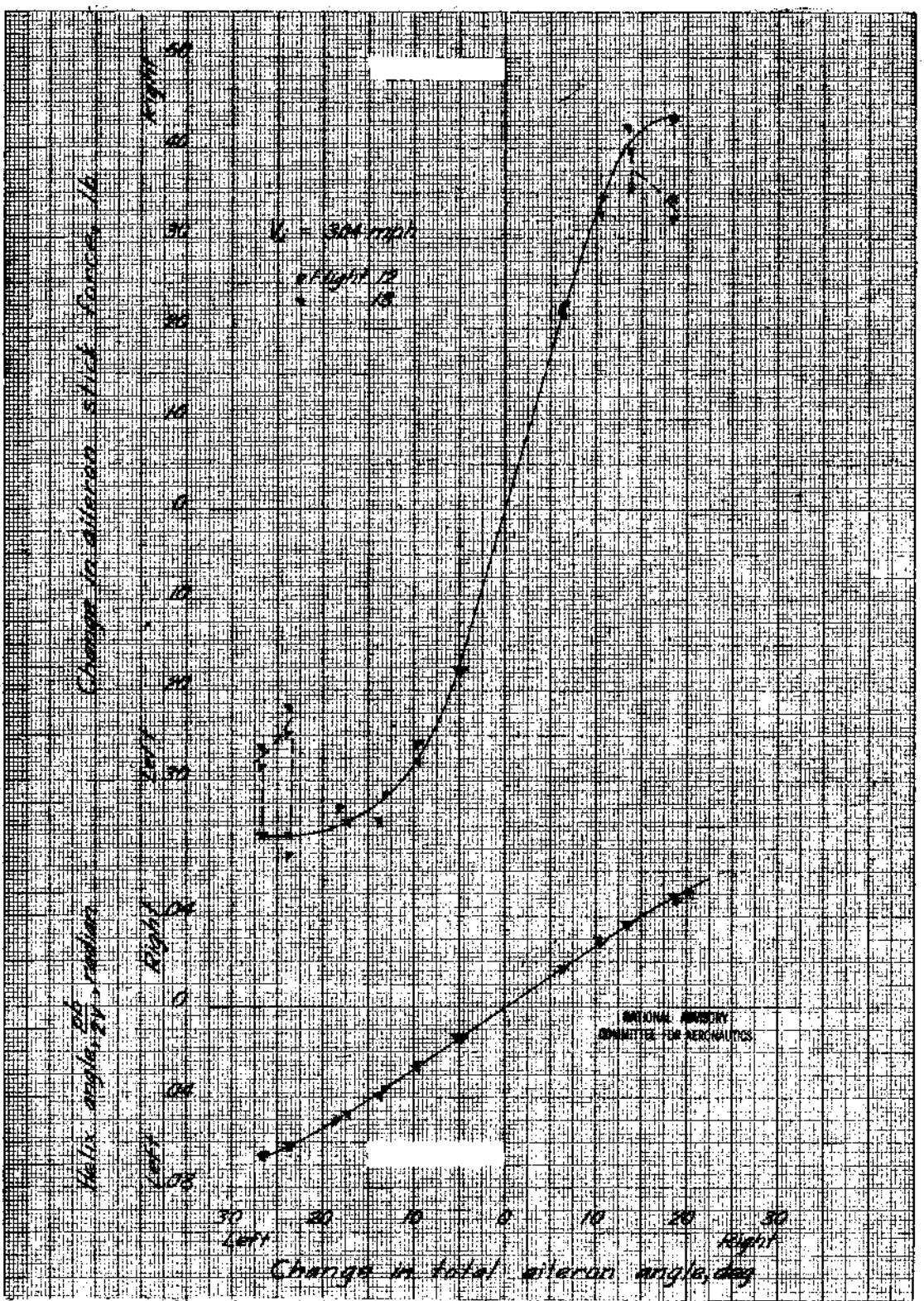

Figure 13 - Aileron rolling effectiveness and stick force characteristics of standard P-40F ailerons as measured in a steady roll at an average indicated airspeed of 304 miles per hour.

L-649

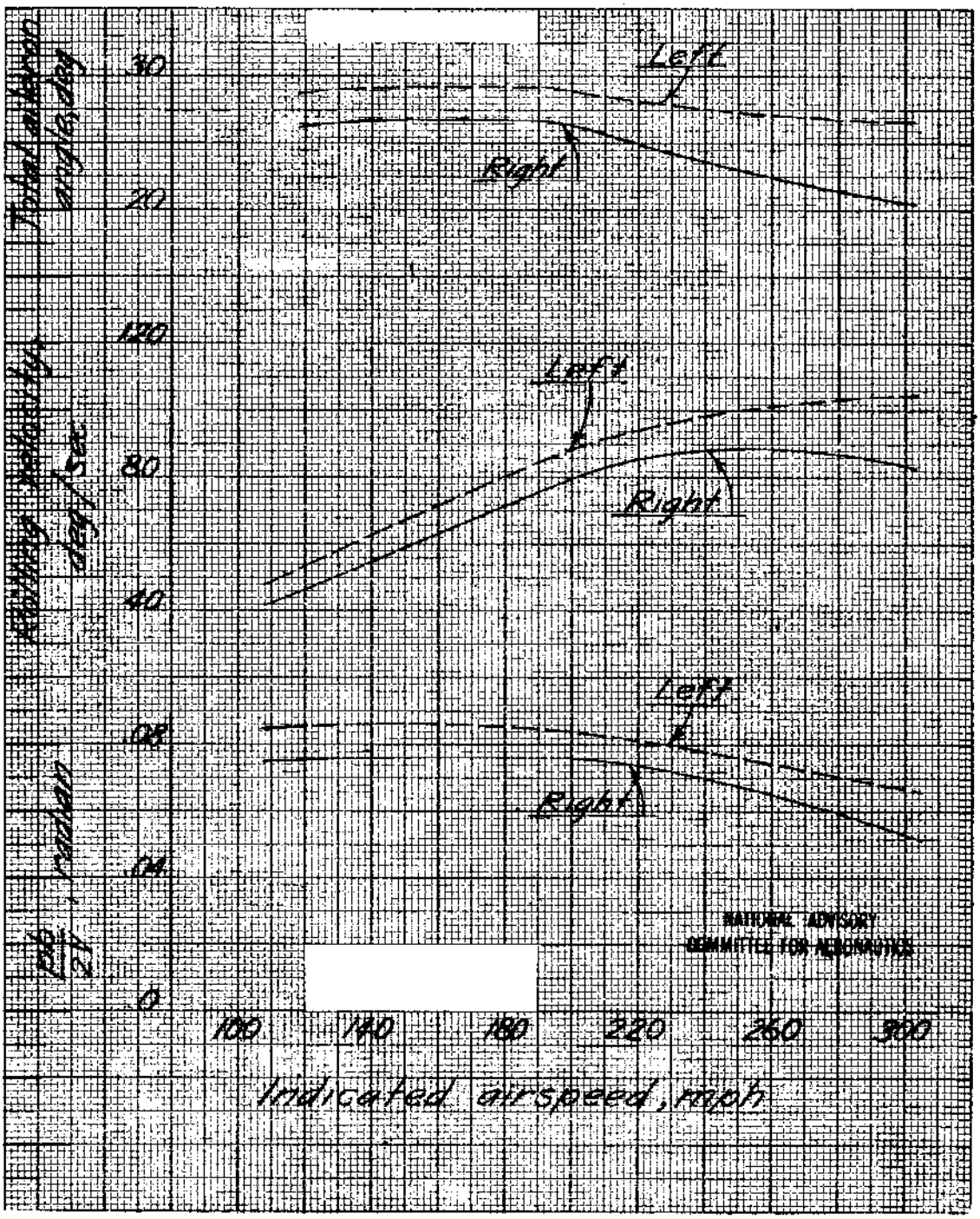

Figure 14 - Variation of rolling characteristics with airspeed at full stick deflection. Maximum stick forces 43 pounds to right and 36 pounds to left.

Figure 15 - Hinge-moment coefficients of standard P-40F ailerons as measured during a steady roll. Left aileron.

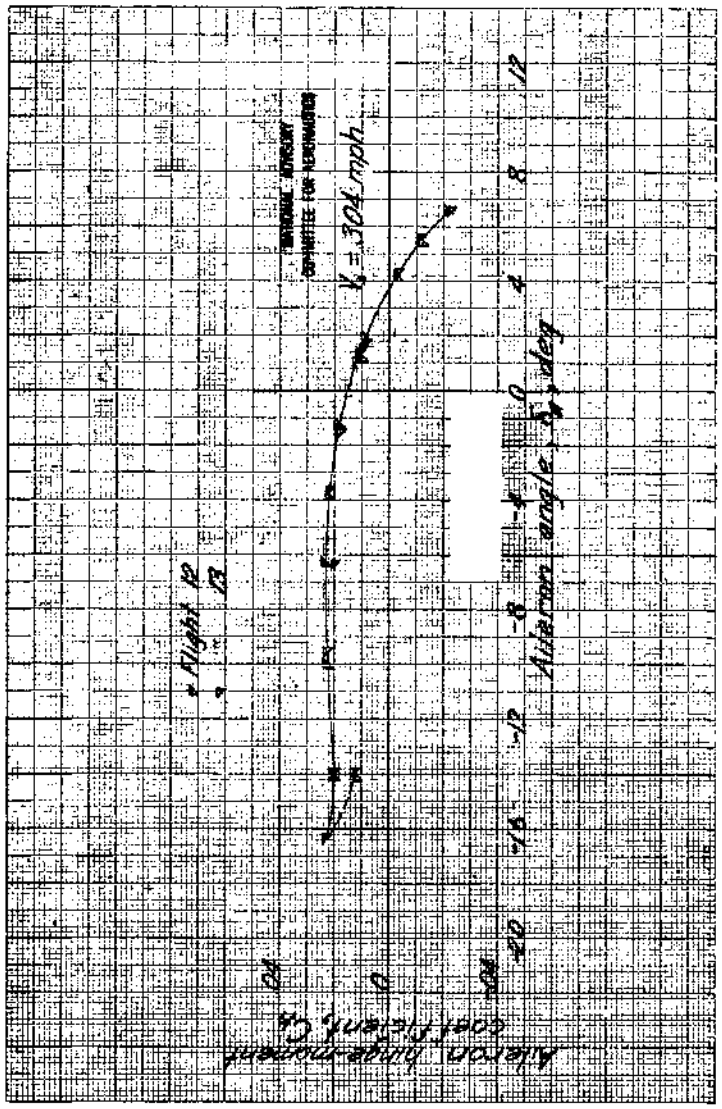

Figure 15 - Concluded.

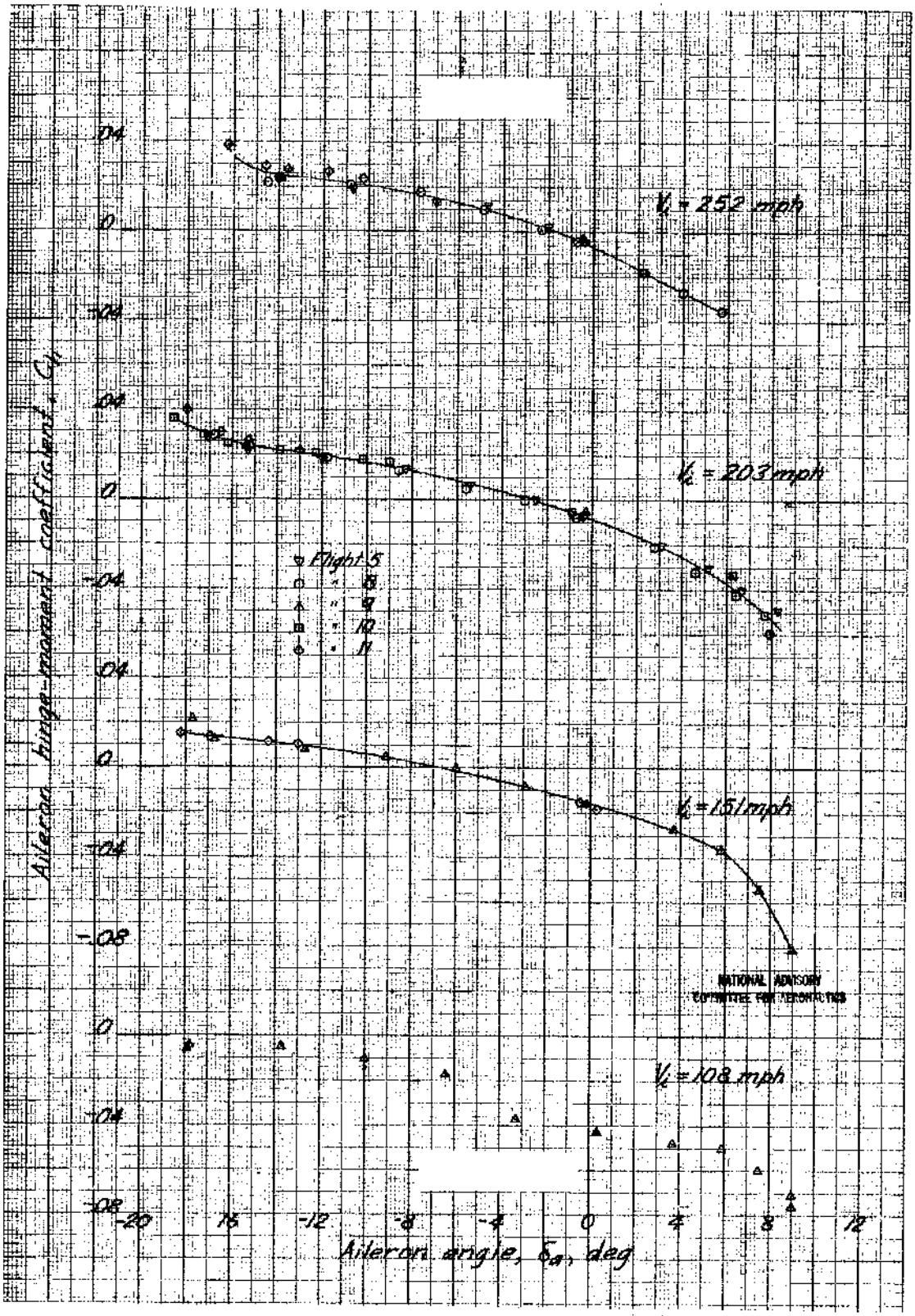

Figure 16 - Hinge-moment coefficients of standard P-40F ailerons as measured during a steady roll. Right aileron.

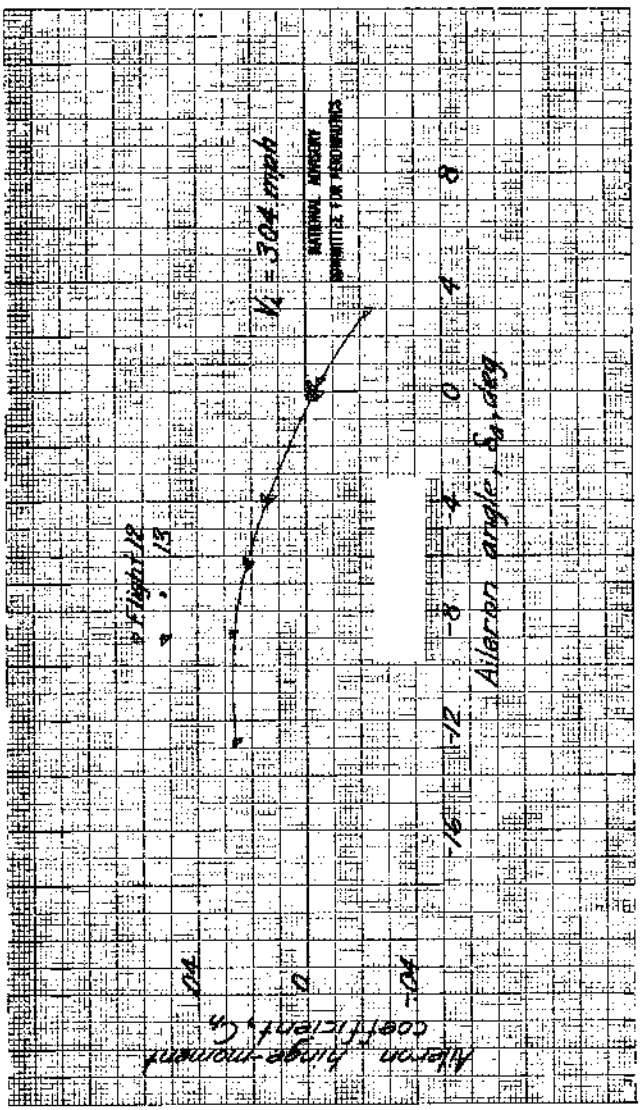

Figure 16 - Concluded.

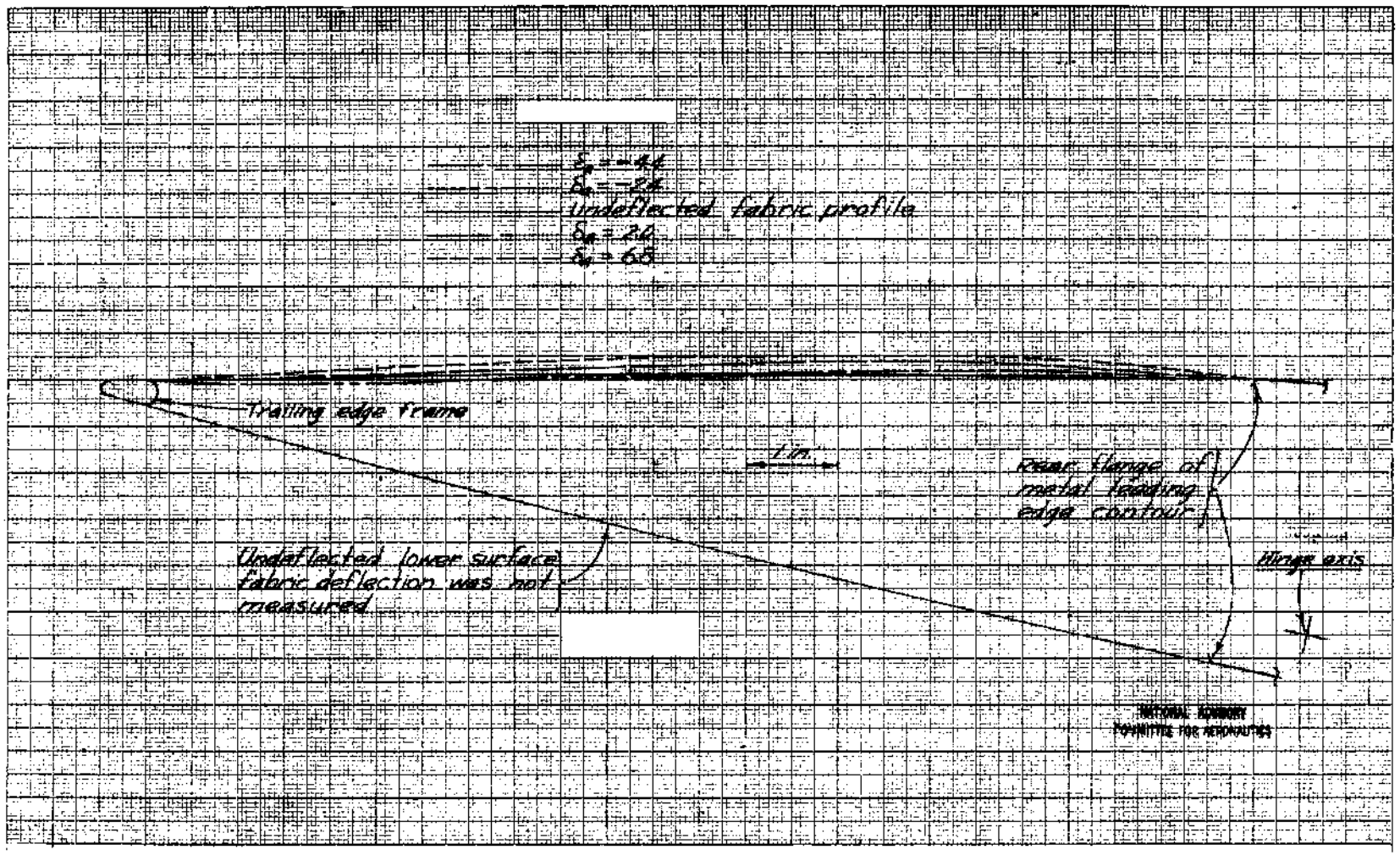

Figure 17 - Change in aileron upper surface contour due to fabric distortion at V_i = 350 miles per hour. Third panel from inboard end of aileron.

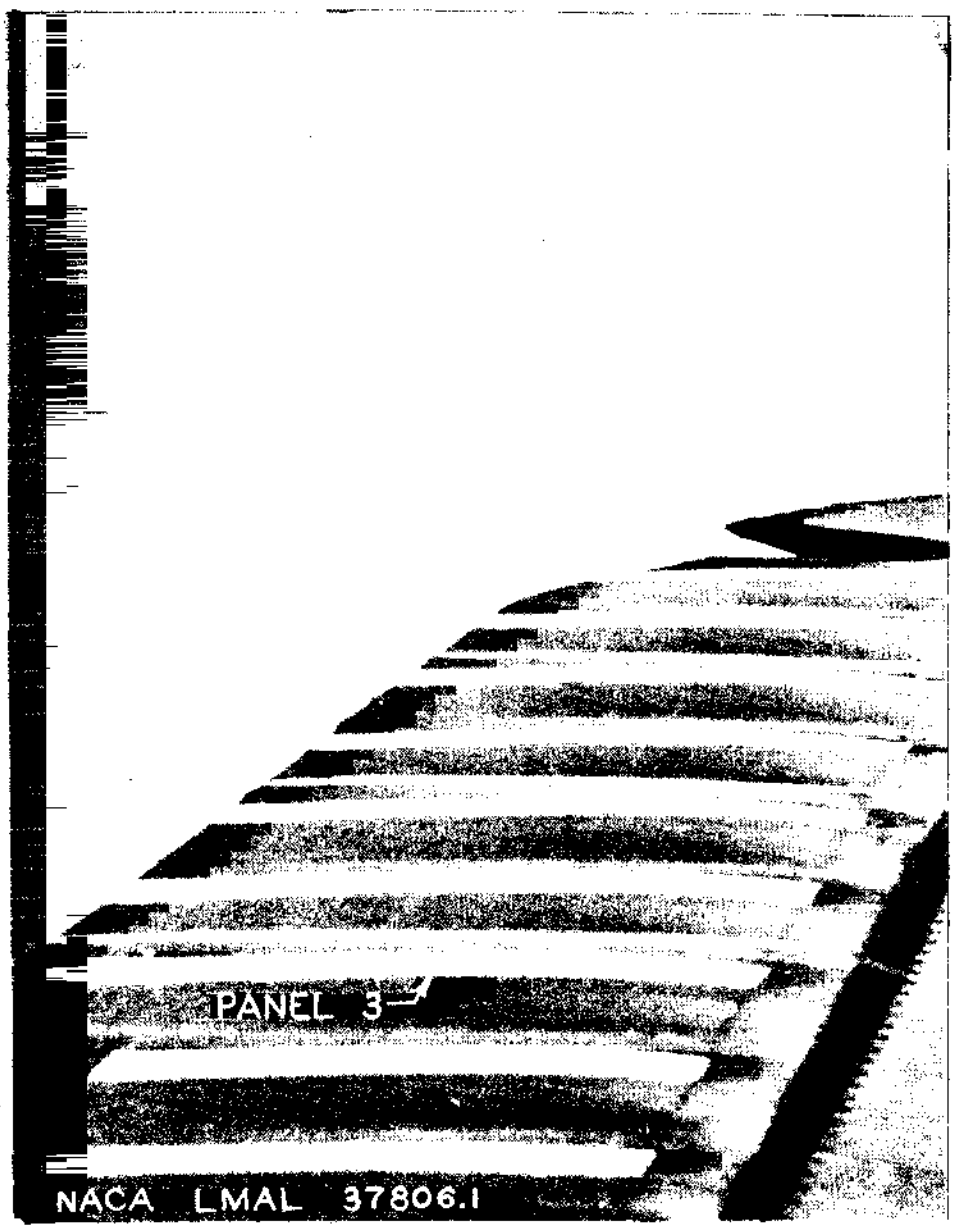

Figure 18.- Typical photograph of left aileron showing fabric bulging at V_i = 350 mph. δ_a = 6.8°. Wide stripes are 2 inches wide with the inboard edge at the center of the panel. Narrow stripes are 1/2 inch wide and mark rib locations.

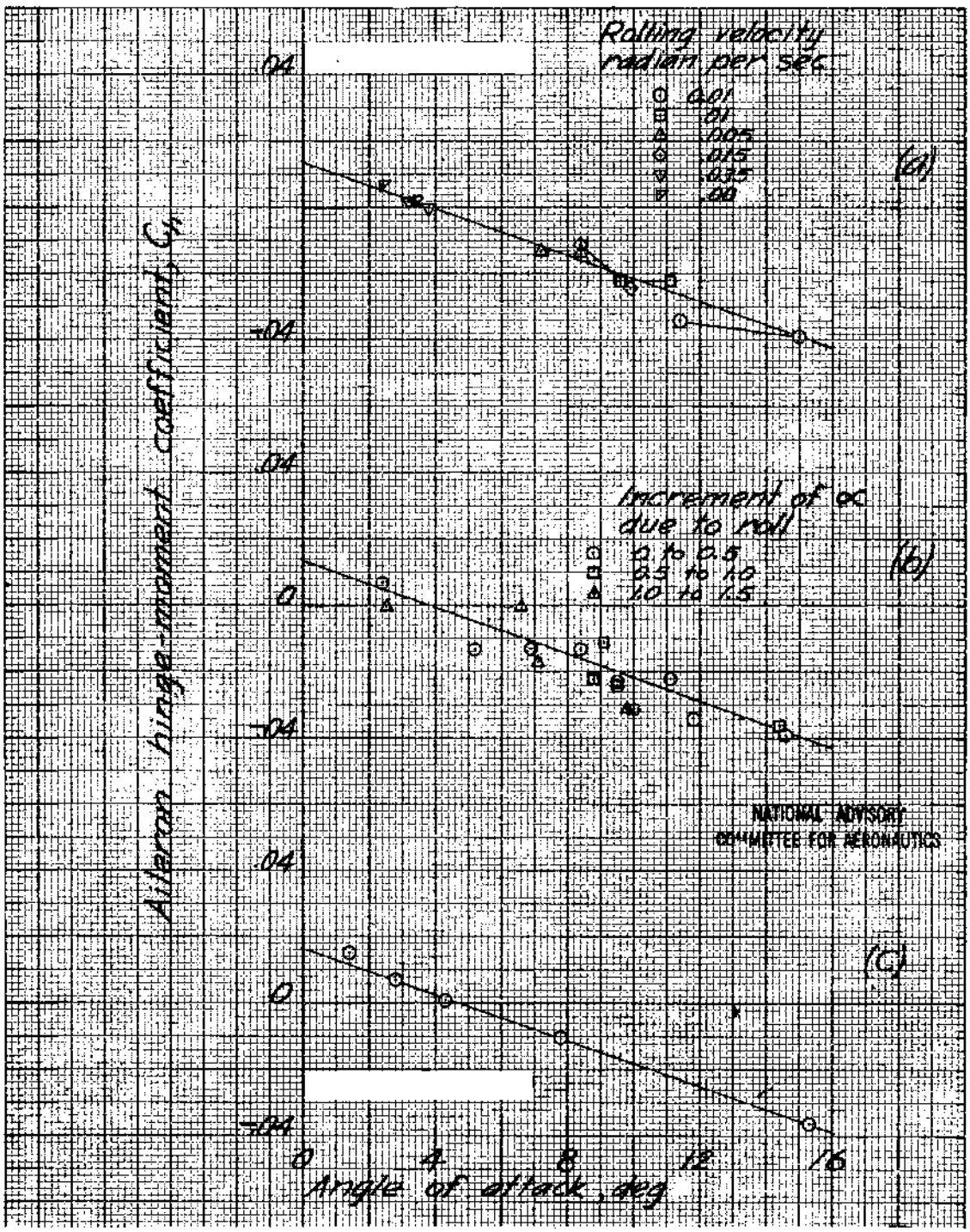

Figure 19 - Variation of the left aileron hinge moment coefficient with angle of attack. Measured in level flight by slowly moving the aileron through neutral.

(a) Each pair of connected points represents equal velocities to left and right.

(b) Angle of attack corrected for the rolling increment of angle of attact at the center of the aileron.

(c) Zero deflection intercepts from figure 14.

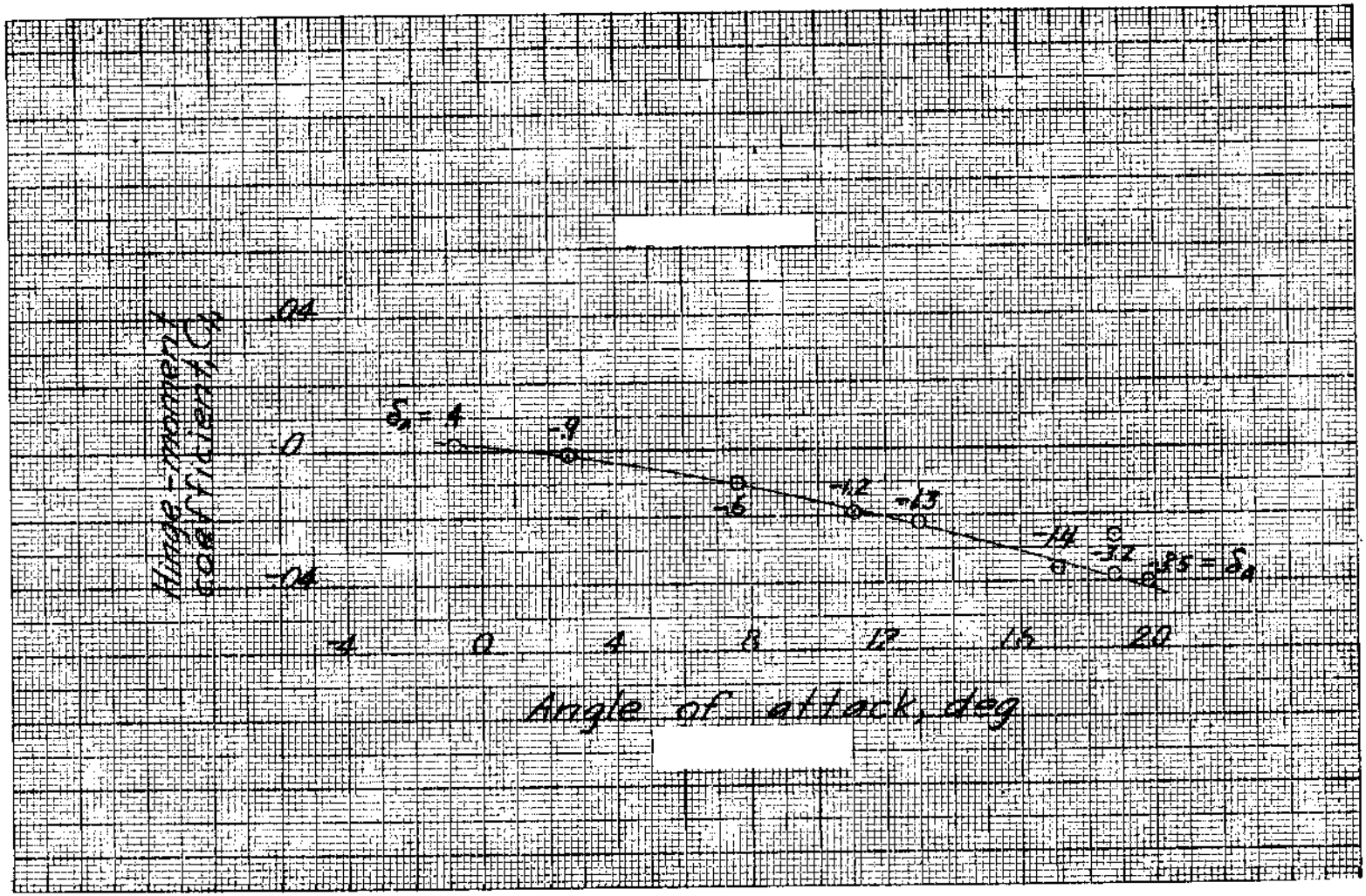

Figure 20 - Variation of the left aileron hinge-moment coefficient with angle of attack as measured in pull-ups and push-downs at 150 miles per hour. Aileron angles are noted at each test point.

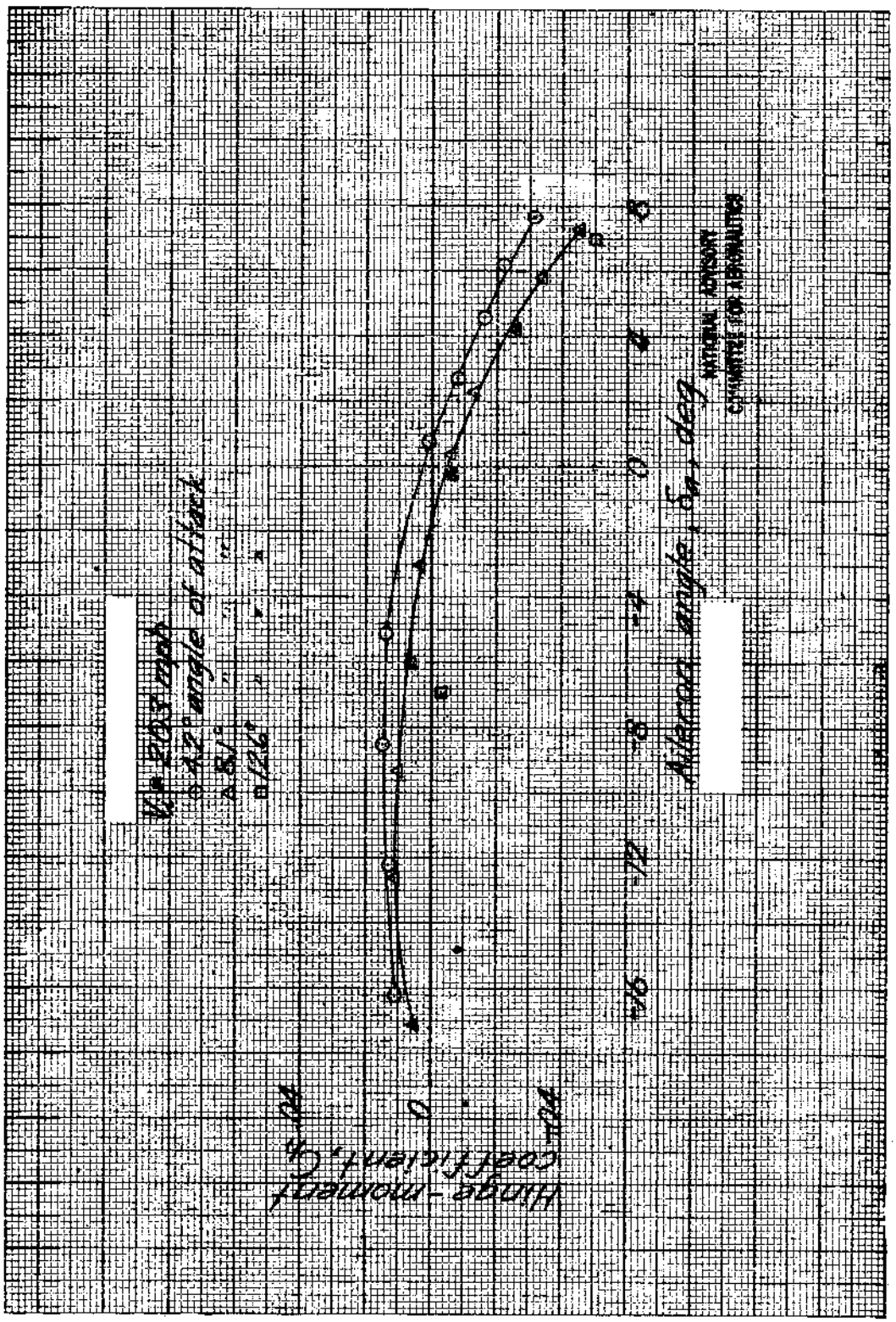

Figure 21 - Variation of the left aileron hinge-moment coefficients with angle of attack as measured in abrupt aileron rolls out of an accelerated turn.

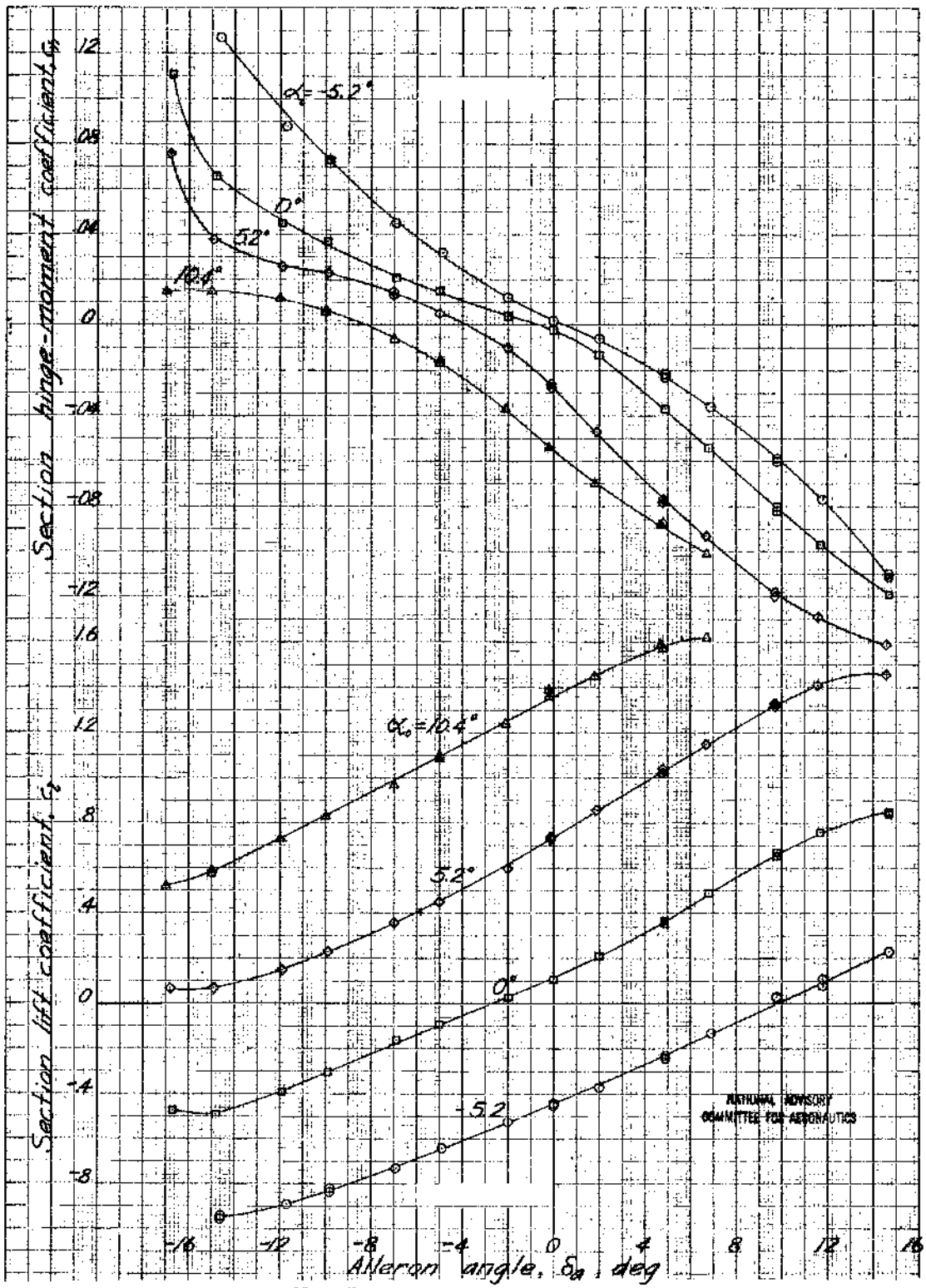

Figure 22. - Variation of section coefficients with aileron angle at various section angles of attack α_o. Impact pressure q_c of 240 pounds per square foot. Data from two-dimensional tests in the Langley Stability Tunnel.

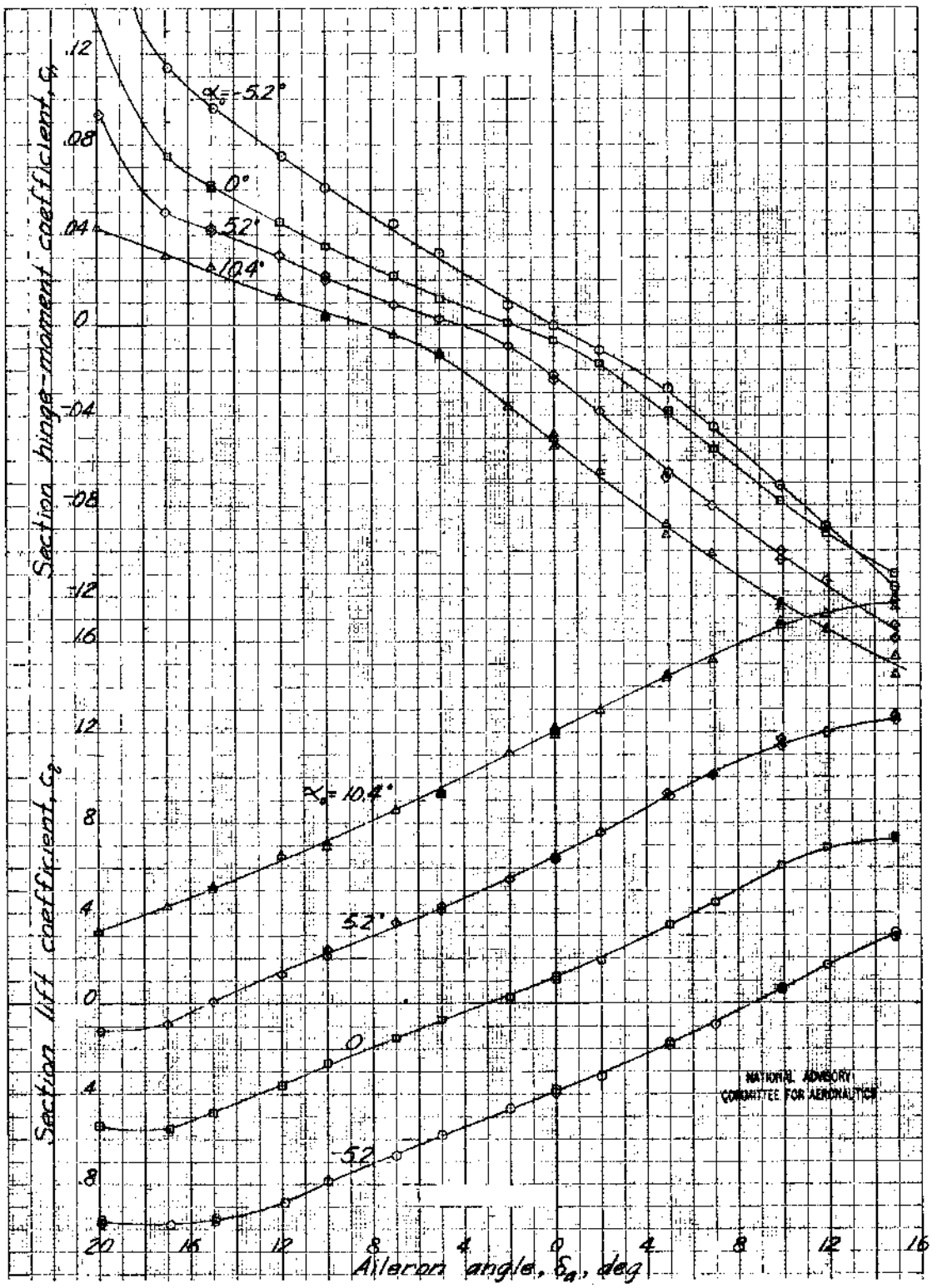

Figure 23. - Variation of section coefficients with aileron angle at various section angles of attack α_0. Impact pressure q_0 of 60 pounds per square foot. Data from two dimensional tests in the Langley Stability Tunnel.

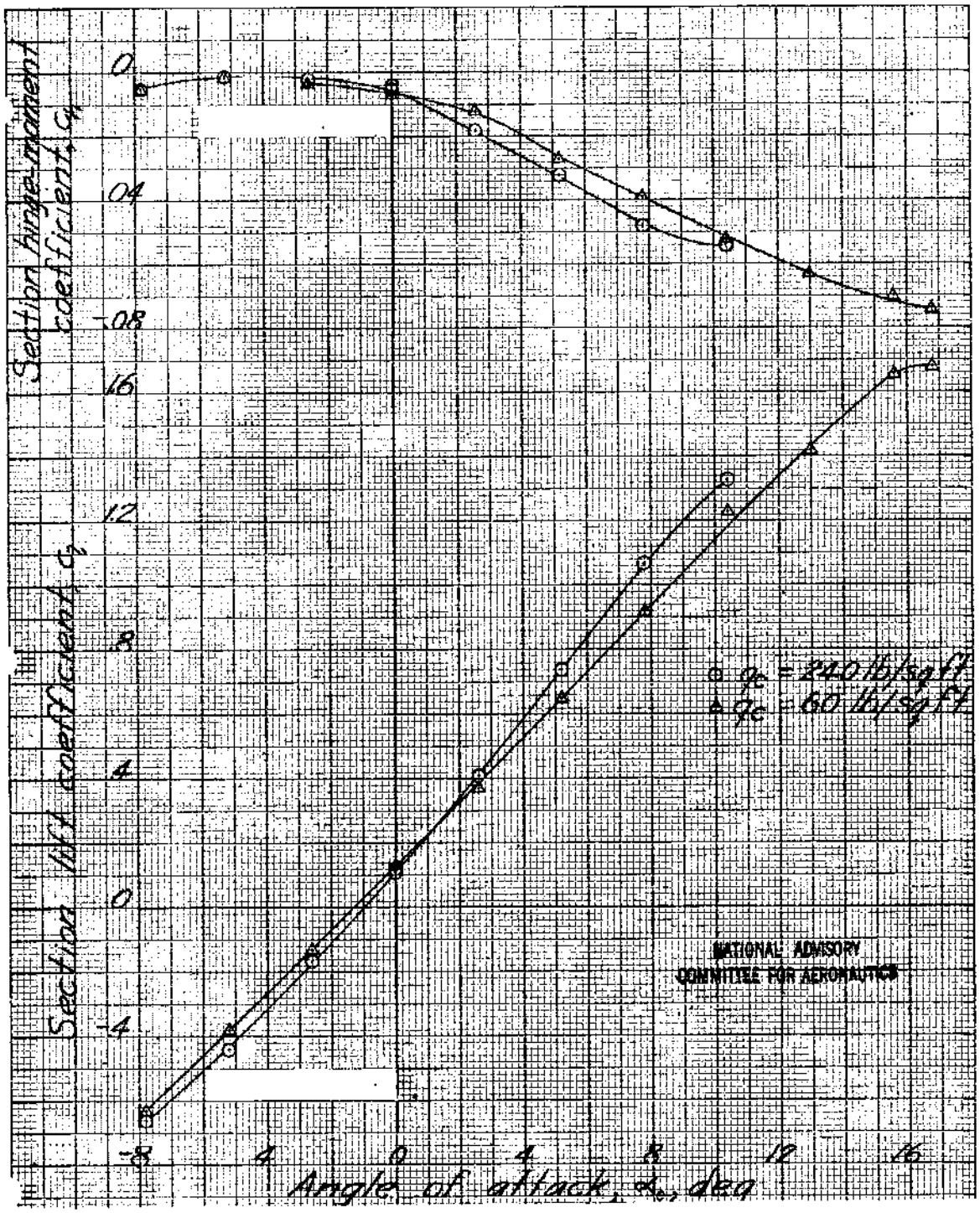

Figure 24. - Variation of section hinge-moment and lift coefficients with section angles of attack α_o at $\delta_a = 0$. Impact pressure q_c of 60 and 240 pounds per square foot. Data from two-dimensional tests in the Langley Stability Tunnel.